Glasnik hemičara i tehnologa Bosne i Hercegovine
Bulletin of the Chemists and Technologists of Bosnia and Herzegovina

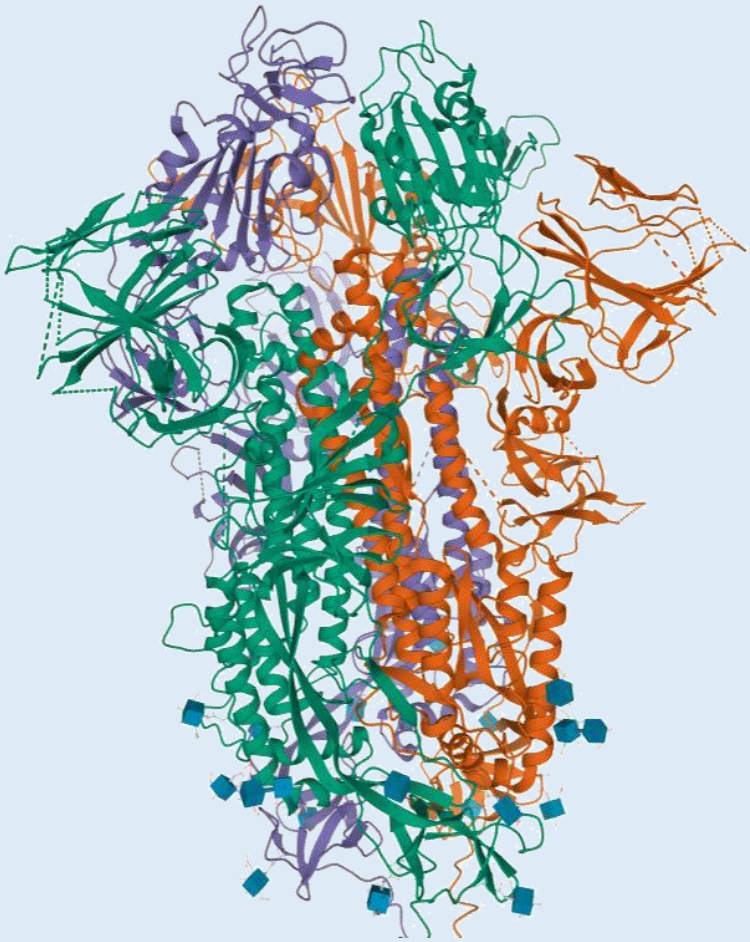

55

December, 2020.

Prirodno-matematički fakultet Sarajevo
Faculty of Science Sarajevo

Glasnik hemičara i tehnologa Bosne i Hercegovine
Bulletin of the Chemists and Technologists of Bosnia and Herzegovina

55

December, 2020.

Prirodno-matematički fakultet Sarajevo
Faculty of Science Sarajevo

Glasnik hemičara i tehnologa Bosne i Hercegovine

Bulletin of the Chemists and Technologists of Bosnia and Herzegovina

Print ISSN: 0367-4444
Online ISSN: 2232-7266

Zmaja od Bosne 33-35, BA-Sarajevo
Bosnia and Herzegovina
Phone: +387-33-279-918
Fax: +387-33-649-359
E-mail: glasnik@pmf.unsa.ba
glasnikhtbh@gmail.com

EDITORIAL BOARD

Faculty of Science Sarajevo
Zmaja od Bosne 33-35, BA-Sarajevo
Bosnia and Herzegovina
Phone: +387-33-279-904 (Administration)
+387-33-279-911 (Executive Editors)
Fax: +387-33-649-359

E-mail: glasnik@pmf.unsa.ba
glasnikhtbh@gmail.com

Dejan Milošević
Department of Physics, Faculty of Science, University of Sarajevo, Sarajevo, Bosnia and Herzegovina
Željko Jaćimović
Department of Chemical Technology, Faculty of Meallurgy and Technology, University of Montenegro, Podgorica, Montenegro
Ljudmila Benedik
Department of Environmental Sciences, "Jožef Stefan" Institute, Ljubljana, Slovenia
Meliha Zejnilagić-Hajrić
Department of Chemistry, Faculty of Science, University of Sarajevo, Sarajevo, Bosnia and Herzegovina
Tidža Muhić-Šarac
Department of Chemistry, Faculty of Science, University of Sarajevo, Sarajevo, Bosnia and Herzegovina
Sabina Gojak-Salimović
Department of Chemistry, Faculty of Science, University of Sarajevo, Sarajevo, Bosnia and Herzegovina
Ismet Tahirović
Department of Chemistry, Faculty of Science, University of Sarajevo, Sarajevo, Bosnia and Herzegovina
Danijela Vidic
Department of Chemistry, Faculty of Science, University of Sarajevo, Sarajevo, Bosnia and Herzegovina
Mustafa Memić
Department of Chemistry, Faculty of Science, University of Sarajevo, Sarajevo, Bosnia and Herzegovina
Andrea Gambaro
Department of Environmental Sciences, Informatics and Statistics, University Ca' Foscari of Venice, Venice, Italy
Institute for the Dynamics of Environmental Processes - National Research Council (CNR-IDPA), Venice, Italy
Dragana Đorđević
Centre of Chemistry - IChTM, University of Belgrade, Belgrade, Serbia
Aida Šapčanin
Department of Natural Sciences in Pharmacy, Faculty of Pharmacy, University of Sarajevo, Sarajevo, Bosnia and Herzegovina
Jože Kotnik
Department of Environmental Sciences, "Jožef Stefan" Institute, Ljubljana, Slovenia
Lucyna Samek
AGH University of Science and Technology, Faculty of Physics and Applied Computer Science, Krakow, Poland
Angela Maria Stortini
Department of Molecular Sciences and Nanosystems, University Ca' Foscari of Venice, Venice, Italy
Ivan Spanik
Institute of Analytical Chemistry, Slovak University of Technology, Bratislava, Slovakia
Mirjana Vojinović Miloradov
Department of Environmental Engineering, Faculty of Technical Sciences, University of Novi Sad, Novi Sad, Serbia
Heike Bradl
Department of Environmental Engineering, University of Applied Sciences Trier, Birkenfeld, Germany
Lea Kukoč-Modun
Department of Analytical Chemistry, Faculty of Chemistry and Technology, University of Split, Split, Croatia
Sanja Ćavar Zeljković
Central Laboratories and Research Support, Centre of the Region Haná for Biotechnological and Agricultural Research, Faculty of Science, Palacký University, Olomouc, Czech Republic;
Department of Genetic Resources for Vegetables Medicinal and Special Plants,Centre of the Region Haná for Biotechnological and Agricultural Research, Crop Research Institute, Olomouc, Czech Republic
Igor Jerković
Department of Organic Chemisty, Faculty of Chemistry and Technology, University of Split, Split,Croatia
Roderick W. Bates
Division of Chemistry and Biological Chemistry, School of Physical and Mathematical Sciences, Nanyang Technlogical University, Singapore, Singapore
Safija Herenda
Department of Chemistry, Faculty of Science, University of Sarajevo, Sarajevo, Bosnia and Herzegovina
Muna Abu-Dalo
Department of Chemistry, Jordan University of Science and Technology, Irbid, Jordan

The journal is published semiannual, and full text version of the papers published are available free of cost at http://www.pmf.unsa.ba/hemija/glasnik.

Bulletin of the Chemists and Technologists has been licensed for indexing in:

Emerging Sources Citation Index (Web of Science, Clarivate Analytics)

CAPlus (Chemical Abstracts Plus):

Academic Search Complete (EBSCO)

Glasnik hemičara i tehnologa Bosne i Hercegovine

Bulletin of the Chemists and Technologists of Bosnia and Herzegovina

Print ISSN: 0367-4444
Online ISSN: 2232-7266

2020
Issue 55

CONTENT

Editorial I

ORIGINAL SCIENTIFIC ARTICLES

Study of uranium bioaccumulation capacity of* Salvia officinalis *L. and* Ocimum basilicum *L. enhanced by citric acid 1-6

Ibragić Saida
Smječanin Narcisa
Hodžić Sara
Ramčić Šadija
Nuhanović Mirza

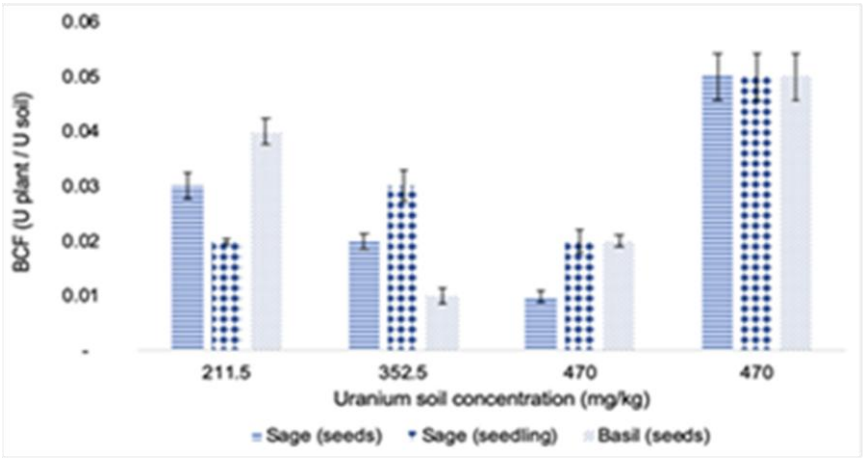

Qualitative and quantitative determination of ligustilide as bioactive marker in apiaceous botanicals 7-12

Durić Kemal
Nikšić Haris
Muratović Samija
Gušić Irma
Korić Emina

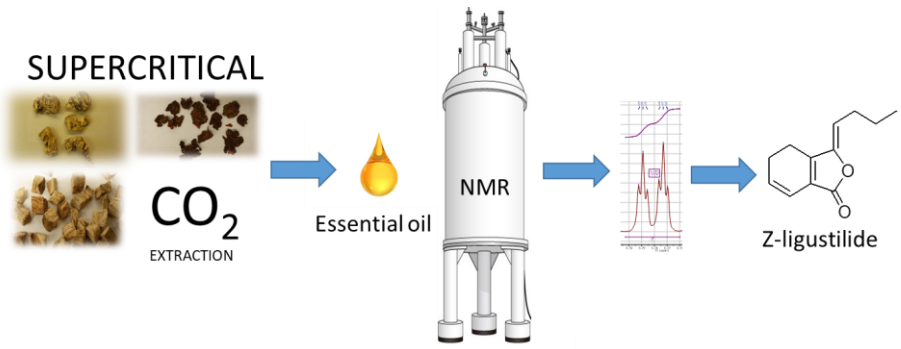

Synthesis and characterization of Fe(III) complex with thiosemicarbazide-based ligand 13-18

Ljubijankić Nevzeta
Galijašević Semira

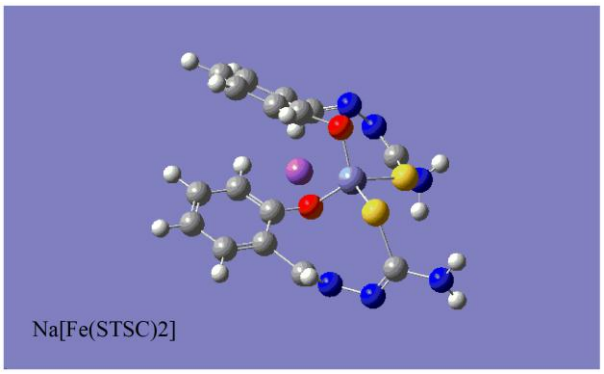

Peroxidase activity of hemoglobin and heme destruction in the presence of hydrogen peroxide and CT-DNA 19-24

Galijašević Semira
Muhidinović Mona
Grizić Selma

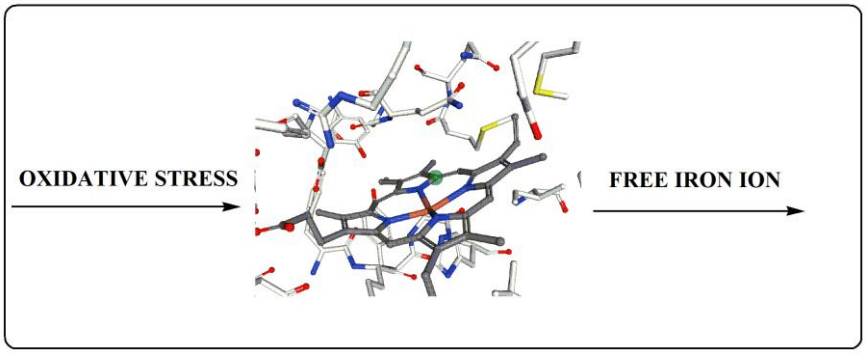

Instructions for authors 25

Sponsors 33

Editorial

Severe acute respiratory syndrome coronavirus (SARS-CoV)-2 is the cause of pandemic that disrupted the world like never before. Though primarily a medical issue, the spectrum of damaged caused by the disease on other aspects of life are numerous. Social connections, economy and general disruption of systems even in the most developed of nations are just some examples of the danger of this pandemic. Ranging in effect from asymptomatic individuals to cases much more severe in nature such as death, the spread of COVID-19 over the world was declared a pandemic by WHO on March 11, 2020. Since then, a numerous research papers, peer reviewed or not has been published in a number of research journals. At his time, thirty nine published papers about novel coronavirus have been retracted including ones published in the most respected journals. As of December, searches for COVID-19 returned 85,02 results in PubMed. At the same time, race to find a relevant treatment to stop pandemic was on the way. In November, BioNtech and Pfizer announced the efficacy of their COVID-19 vaccine based on mRNA technology.

According to US Food and Drug Administration Pfizer's vaccine is composed of active ingredients, salts and sucrose. Active Ingredients are nucleoside-modified messenger RNA -1273 (mRNA) encoding the viral spike glycoprotein (S) of SARS-CoV-2. Spike glycoprotein is the one that latch to the cells and gains entry allowing the virus to function inside the cell. Vaccine contains modified mRNA sequence that codes only for spike glycoprotein. It is packed in complex positively-charged lipids, in order to make it more stable and resistant to RNase-catalyzed degradation. When applied, lipid particles packed with modified mRNA are endocytosed, and its content release in the cytosol, where the mRNA is translated into antigenic proteins causing immune system to produce neutralizing antibodies. Lipids nanoparticles are added to encase the mRNA.

The first lipid structure is (4-hydroxybutyl)azanediyl)bis(hexane-6,1-diyl)bis(2-hexyldecanoate), (Patent number ALC-3015), then 2-[(polyethylene glycol)-2000]-N,N-ditetradecylacetamide (patent number ALC-0159), 1,2-distearoyl-snglycero-3-phosphocholine (DPSC) and cholesterol.

Salts such as potassium chloride, monobasic potassium phosphate, sodium chloride, basic sodium phosphate dehydrate are added for pH control. The one of the draw back of the vaccine is a need to be kept at low temperature (-73 °C) and use within several days after thawed.

These vaccines that are so widely needed now more than ever, are a great success in regards to molecular medicine and biotechnology. It is also important to note what an achievement this is for nanomedicine given the absence of recognition for this field. Due to the characteristics and nature of delivering genetic material, nanomedicine is of great importance with all its principles. These biocompatible engineered materials are necessary for the protection of drug cargos and offer biodistribution and intracellular localization. Targeting cancer cells with nanotechnology-designed drugs and precise delivery has been in works for a while. This line of events might help with development of nanomedicine and a new strategies for the treatment of a different diseases

Editors

Glasnik hemičara i tehnologa Bosne i Hercegovine

Bulletin of the Chemists and Technologists of Bosnia and Herzegovina

2020

55

Print ISSN: 0367-4444
Online ISSN: 2232-7266

Original Scientific Article
DOI: https://doi.org/10.35666/ghtbh.2020.55.01
UDC: 544.58:623.459.86

1-6

Study of uranium bioaccumulation capacity of *Salvia officinalis* L. and *Ocimum basilicum* L. enhanced by citric acid

Ibragić, S., Smječanin, N., Hodžić, S., Ramčić, Š., Nuhanović, M.*

Department of Chemistry, Faculty of Science, University of Sarajevo, Zmaja od Bosne 33-35, Sarajevo, B&H

Article info
Received: 05/03/2020
Accepted: 28/07/2020

Keywords:
Uranium phytoextraction
Sage
Basil
Citric acid

***Corresponding author:**
Mirza Nuhanović
E-mail:mirzanuhanovic1.0@gmail.com
Phone: 00 387-33-279-865

Abstract: Plants possess various intrinsic mechanisms necessary to accumulate and either sequester or detoxify soil contaminants, including radionuclides. The aim of this study was to determine the bioconcentration factor of two fast growing plants *Salvia offlicinalis* L. (sage) and *Ocimum basillicum* L. (basil) that were cultivated in pH neutral soils artificially contaminated with three different concentrations of uranium (211, 352 and 470 mg/kg). The efficiency of citric acid was evaluated with respect to the enhancement of the phytoextraction process. The results showed that the bioconcentration factor did not differ significantly between the selected species (0.01 - 0.03). Citric acid was added in doses (50 mL, 30 mM) until the first effects of uranium phytotoxicity appeared. After four doses of citric acid, the bioconcentration factor reached 0.05 for both plants. The increase of uranium content taken up by the respective plants was more pronounced. Thus, the uranium content of sage grown in contaminated soil (470 mg/kg) increased from 6.03 to 21.28 mg/kg in citric acid-treated soil. The data obtained confirmed the efficiency of citric acid in enhancing phytoextraction of uranium and further suggest that even plants of a rather small biomass can be useful in phytoremediation given the appropriate treatment through induced phytoextraction with appropriate chemical agents.

INTRODUCTION

Having the ability to absorb and accumulate metals, plants have become valuable tools in controlling or remediating environmental contamination. Plant-assisted remediation of soil containing radionuclides generally occurs through one of the following mechanisms: phytoextraction, rhizofiltration, phytovolatilization or phytostabilization (Duschenkov, 2003). Apart from being a low-cost alternative to engineering-based remediation methods such as excavations, phytoremediation allows *in situ* treatment of soil and it is a technique that can be used as a long-term treatment (Gavrilescu *et al*., 2009).

Numerous, and predominantly terrestrial plant species have been investigated for their capacity to accumulate uranium such as *Brassica* sp., *Trifolium* sp., *Helianthus annuus* L., *Zea mays* L., (Malaviyaand Singh, 2013). Among 34 species that have been screened by Shahanadeh and Hossner (2002a), *Brassica juncea* (L.) Czern. and *Helianthus annuus* L., proved to be particularly suitable for phytoremediation of uranium.

The bioaccumulation of uranium depends not only on the plant species and its cultivation conditions, but also on the soil composition, soil pH, coexisting ions, contamination exposure, amendments and the very uranium speciation (Claus *et al*., 2007; Schindler *et al*., 2015; Černe *et al*., 2018; Meng *et al*., 2018; Khan, 2020). Various types of amendments and many methods, including agricultural strategies, are currently being used to improve phytoremediation processes (Rostami *et al*. 2019; Li *et al*., 2018). Low molecular organic acids, in particular citric acid (CA), have been used in many studies to enhance plant uptake of uranium during phytoextraction (Shahandeh and Hossner, 2002a). The aim of this work was to investigate and compare the bioaccumulation capacity of two fast growing plant species sage and basil and to evaluate the plants' responses to the chosen amendment - citric acid.

EXPERIMENTAL

Soil contamination

The used soil was commercially obtained. According to the declaration it contained 64% black peat, 34% white peat and 2% clay. The heavy metal content (mg/kg) was as follows: Cd<0.1, Cr<8.0, Cu<9.0, Hg<0.1, Pb<10.0, Zn<15.0. The soil was thoroughly homogenized and air dried for 10 days at room temperature.

The soil was portioned and irrigated using aqueous solutions of uranyl nitrate hexahydrate. Thus, three sets of soil samples were prepared containing 450 mg/kg, 700 mg/kg and 1000 mg/kg uranyl nitrate hexahydrate which corresponds to 211.5 mg/kg, 352.5 mg/kg and 470.0 mg/kg uranium. The soil was homogenized every two days for two weeks, after which it was used in pot experiments to cultivate sage from seeds and seedlings and basil from seeds. Non-contaminated soil was used as a control.

Determination of soil pH

The pH was determined in non-contaminated soil in triplicates. Soil samples (5 g) were suspended in 50 mL water (pH in H_2O) and in 50 mL 1 M KCl (pH in KCl), periodically mixed for 1 hour and the pH was measured using a glass electrode.

Plant culture

Sage and basil seeds were commercially obtained (producer: Royal seeds) and used to grow seedlings in non-contaminated soil for 8 weeks. After that period, the sage seedlings were transferred into pots containing cca. 300 g soil and watered with aqueous solutions of uranium every other day. At the same time, sage and basil seeds were planted into the already contaminated soil. Thus, the seedlings were allowed to grow for 8 weeks. To evaluate the effects of additive on bioaccumulation, plants grown in the highest uranium concentration were watered with 50 mL of 30 mM citric acid every other day, 4 times in total.

Soil analysis

Soil samples were subjected to acid digestion according to EPA method (3050B). Each air-dried soil sample (3g) was transferred into a vessel and mixed with 21 mL conc. HCl, 7 mL conc. HNO_3 and 1 mL distilled water. The suspension was left overnight (16 hours) at room temperature before another 5 mL HNO_3 were added, and heated. After cooling down, 2 mL of distilled water and 3 mL 30% H_2O_2 were added to the suspension. To achieve complete oxidation, the suspensions were additionally heated and small volumes of 30% H_2O_2 were added gradually. The suspensions were then filtrated, transferred into measuring flasks (50 mL) and filled up to the mark with distilled water.

Plant analysis

The harvested plant samples (roots and areal parts) were washed with distilled water and soil particles were removed from the roots by immersing them into a 0.5 M$CaCO_3$ solution for 3 hours. Then, the roots were washed out with distilled water again, excess of water on the surface was wiped off with absorbent paper and the plants were dried in an oven at 70ºC to constant weight. After weighing the biomasses, the plant material was pulverized into fine powder. The plant samples were analyzed by weighing 0.45 g plant powder and leaving it overnight suspended in 3 mL conc. HNO_3. Then, the suspension was heated for 1 h at 125ºC, 2 mL 30% H_2O_2 and 0.5 mL distilled water were added, while continuing heating and adding more H_2O_2 until the solution became clear. The sample was filtrated and filled with distilled water to 10 mL.

ICP-MS Analysis

Soil and plant sample solutions were analyzed in triplicate using mass spectrometry with inductive coupled plasma (ICP-MS Agilent 7700x) and the obtained data processed with Agilent Mass Hunter. Operating parameters for the ICP-MS in He mode were as follows: voltage power (RF) 1550 W; sample depth 7-10 mm, points per peak 3; resolution at 10% peak's height 0.65 - 0.8; carrier gas 1.01 - 1.11 L/min; He gas 2.5-6 mL/min; S/C temperature 2ºC; nebulizer pump 0.1 rps.

RESULTS AND DISCUSSION

The soil pH, determined before the contamination process, was in the neutral range. The pH measured in water was 6.98±0.05 and 6.70±0.03 measured in water and KCl, respectively.

Table 1: Uranium concentration in analysed soil and plant samples (mg/kg) determined by ICP-MS

Contaminated soil	Sage (whole plant)		Basil (whole plant)
U (mg/kg)	**Seeds**	**Seedlings**	**Seeds**
211.5	7.1 ± 0.5 (6.6 – 7.6)	3.6 ± 0.1 (3.5 – 3.7)	7.8 ± 0.5 (7.3 – 8.3)
352.5	6.6 ± 0.5 (6.1 – 7.1)	11.4 ± 1 (10.5 – 12.4)	3.5 ± 0.5 (3.2 – 4.1)
470.0	6.0 ± 0.5 (5.6 – 6.5)	9.8 ± 1 (8.8 – 10.8)	8.0 ± 0.5 (7.5 – 8.5)
470.0 + CA	21.3 ± 2 (23.2 – 25.0)	21.6 ± 2 (19.6 – 23.6)	23.1 ± 2 (19.2 – 22.9)

* The results are expressed as Mean value ± SD

Due to the relatively short growth period of nine weeks and the low biomass of the selected plants that did not exceed 0.5 g dry weight, the uranium concentration was determined as a total present in root and areal parts (stem and leaves). As can be seen from Table 1, the uranium concentration in sage and basil grown from seeds does not differ much, except for samples grown in 352.5 mg/kg U contaminated soil. Similarly, a significant difference between uranium concentrations in plants grown from seeds and those from transplanted seedlings was not established.

The bioconcentration factor (BCF), also known as plant transfer factor (TF), measures the bioaccumulation or bioconcentration capacity of the whole plant to remove contaminants and is calculated according to the equation (Dushenkov, 2003):

$$BCF = \frac{plant\ uranium\ content\ (mg/kg)}{soil\ uranium\ content\ (mg/kg)}$$

Most of the studies (Wang *et al*.,2018; Mihalík *et al*. 2010), represent the BCF of the shoot and root system separately, however the BCF values of this study refer to the uranium content in the whole plant / uranium content in soil upon contamination, on dry weight basis (presented in Fig. 1).

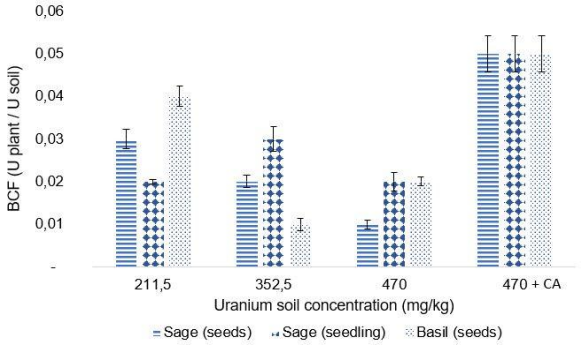

Figure 1: Bioaccumulation of uranium in roots and areal parts of sage and basil grown from seeds and seedlings.

The aim and purpose of phytoextraction is maximum extraction of contaminants - a process determined by many factors. The efficiency of that process is often evaluated by the BCF. In the case of uranium, the BCF is small and typically in a range between 0.0002 - 0.38 for shoots and between 0.007 - 8.1 for roots (Malaviya and Singh 2013). Leafy vegetables generally show higher BCFs, followed by root, fruit and grain crops (Vandenhove *et al*., 2001). The current contribution aimed to explore the capacity of sage and basil, two fast growing medicinal plant species from the Lamiaceae family, to accumulate uranium with and without any amendment addition. The plants grown from seeds and the transplanted seedlings were exposed equally long to the different uranium concentrations. Changes observed in the uranium content in the whole plants grown from sage seeds (7.05 to 6.03 mg/kg) imply a gradual decline with the increase of uranium concentrations in the soil. In the case of sage grown from seedlings, the U content in the plant increased more than 3-fold in the soil contaminated with 352.5 mg/kg U compared to the soil contaminated with 211.5 mg/kg uranium. The same pattern is reflected in the BCF values, as well. A nonlinear correlation between the uranium soil concentration and BCF has been reported by Alsabbagh and Abuqudaira (2017) who concluded that while the uranium removal percentage values were close, they did not directly depend on the three different soil concentrations to which the sunflower plants were exposed during the 10 weeks of the pot experiment. Wang *et al*., (2018), on the other hand, demonstrated an inversely proportional relationship. They conducted a pot experiment sawing *Boehmeria nivea* seeds in contaminated soil, and for the three uranium concentrations of 175.275 and 485 mg/kg the BCF was 1.834, 1.084 and 0.295, respectively. *Helianthus annuus* L. is one of the most extensively analysed plant species for uranium bioaccumulation and there are reports of uranium content in whole plants such as 44 mg/kg where C uranium in soil = 480 mg/kg (Mihalík*et al.* 2010) or cca. 16 mg/kg where C uranium in soil = 253 mg/kg (Alsabbaghand Abuqudaira, 2017). In this study, the uranium content in sage and basil at the initial soil concentration (211.5 mg/kg) was 7.05 mg/kg and 7.79 mg/kg, respectively which is remarkable considering the differences in biomass and morphology of the selected plants compared to sunflower.

The results of this study (Fig. 1.) confirmed the effectiveness of CA on the enhancement of uranium phytoextraction and consequently on the BCF. The newly created conditions after CA treatment caused a 3-fold increase in the uranium concentration in sage and basil grown from seeds. This effect was even more pronounced in sage grown from seedlings where the initial uranium concentration rose from 3.6 to 21.56 mg/kg. Interestingly, the BCF reached the value of 0.05 for both sage and basil, regardless of the cultivation type. Most probably the uranium in the complex with CA improved the metal uptake by both plants. Organic acids, can directly complex cations, change the soil pH, and increase the uranium mobility in the soil (Vandenhove *et al*., 2001; Shahnadeh and Hossner, 2002a; Duquène *et al*., 2008). Ideally, phytoextraction amendments should improve plant accumulation of the targeted metal but also stay environmentally friendly (Parra *et al*., 2008). Citric acid as a natural alternative to synthetic chelators has a shorter environmental half-life, it is biodegradable, less toxic and can be obtained at relatively low-cost (Malaviya and Singh 2013). The results of this study are in line with literature findings (Li Chen *et al.* 2019; Hu *et al.*2019.). One of the early studies (Huang *et al.* 1998) showed that shoot U concentrations of *Brassica juncea* (L.*)* Czern. and *Brassica chinensis* L. grown in a U-contaminated soil (750 mg/kg) increased from less than 5 mg/kg to more than 5000 mg/kg in citric acid-treated soils. Chang *et al.* (2005) expanded their research evaluating the CA effects on uranium accumulation in aboveground biomass of *Brassica juncea* (L.*)* Czern, *Brassica chinensis* var. *oleifera*, *Brassica napus* L. var. *napus* and *H. annuus* L. considering two soil types. For all investigated plants, CA was efficient in boosting the bioaccumulation of uranium. Mihalík *et al*., (2010) compared the effectiveness of a single and repeated dose of CA using *H. annuus* and *Salix* spp. for phytoremediation. A single treatment with 300 mL 80 mM CA was only effective for *Salix* spp., however after 5 doses the uptake of uranium increased in both plants. In our experiment, CA was used in four doses (50 mL 30 mM CA, every other day) after which the treatment was stopped because plant withering became apparent. The different uranium soil concentrations visibly reduced the growth rate of the selected plants; however, the toxic threshold of soil uranium became evident after the repeated CA additions. Thus, it is most probably the synergistic effects of uranium and CA that caused the negative effects, which is not surprising as several other authors reported inhibited plant growth upon CA addition (Vandenhove *et al*., 2001; Shahandeh and Hossner, 2002a, b; Lesage *et al*., 2005).

To the best of our knowledge, the uranium bioaccumulation capacity of sage and basil has not been previously investigated and a direct comparison of the BCF results is therefore not at hand. A comparison to other species would need to take into account a rich set of parameters such as plant species and its mechanisms to sequester unwanted contaminants, biomass, uranium

concentration and exposure time, uranium speciation, soil type, pH, amendment and its concentration and whether BCF is calculated for the whole plant, root system or shoot system. On these grounds, we restricted to the results obtained by this study and concluded that basil and sage are equally suitable for phytoremediation purposes and that their capacity for uranium bioconcentration can be significantly increased with the addition of an appropriate amount of CA, which will not induce the uranium phytotoxicity. It is known that the soil pH must decline below 5.0 to effectively transport uranium to the shoots due to the predominance of the soluble uranyl cation (Ebbs *et al*., 1998). In our study, the soil pH was in the neutral range which may explain the low uranium concentrations determined in the plants prior to the addition of CA. The type of soil and its properties will play an additional role in the mobility, binding capacity and chemical reactivity of uranium and thus affect the overall bioaccumulation capacity of plants (Yan and Luo, 2015).

CONCLUSIONS

The search for plants that have the highest potential towards uranium bioconcentration as well as the optimal conditions are essential for successful soil remediation of this radionuclide. Although the obtained results are based on a pot experiment, it has been clearly demonstrated that sage and basil grown from seeds have similar BCF values that were not in a linear correlation with the uranium concentration in the soil. After the addition of four doses of citric acid, when the first signs of phytotoxicity became visible, the BCF has increased to 0.05 for both plant species. The low uranium content in whole plants prior to the addition of CA may be partially explained by the neutral pH of the soil. In summary, this study has provided first data on the potential of sage and basil for uranium bioaccumulation and demonstrated that even plants with a small biomass may be utilized for phytoremediation in combination with suitable amendment agents.

REFERENCES

Agarwal, P., Agarwal, N., Gupta, R., Gupta, M., Sharma, B. (2016). Antibacterial activity of plants extracts against methicillin-resistant *Staphylococcus aureus* and vancomycin-resistant *Enterococcus faecalis*. *Journal of Microbial and Biochemical Technology, 8*, 404-407.

Alsabbagh, A. H., Abuqudaira, T. M. (2017). Phytoremediation of Jordanian uranium-rich soil using Sunflower. *Water, Air, & Soil Pollution*, *228*(6), 219.

Chang, P., Kim, K. W., Yoshida, S., Kim, S. Y. (2005). Uranium accumulation of crop plants enhanced by citric acid. *Environmental Geochemistry and Health*, *27*(5-6), 529-538.

Chen, L., Wang, D., Long, C., & Cui, Z. X. (2019). Effect of biodegradable chelators on induced phytoextraction of uranium-and cadmium-contaminated soil by *Zebrina pendula* Schnizl. *Scientific Reports, 9*.

Claus, D., Dietze, H., Gerth, A., Grosser, W., Hebner, A. (2007). Application of agronomic practice improves phytoextraction on a multipolluted site. *Journal of Environmental Engineering and Landscape Management, 15*(4), 208–212.

Černe, M., Smodiš, B., Štrok, M., Jaćimović, R. (2018). Plant Accumulation of Natural Radionuclides as Affected by Substrate Contaminated with Uranium-Mill Tailings. *Water, Air, & Soil Pollution, 229(*11*),* 371.

Duque`ne, L., Tack, F., Meers, E., Baeten, J., Wannijn, J., Vandenhove, H. (2008). Effect of biodegradable amendments on uranium solubility in contaminated soils. *Science of the Total Environment, 391*(1), 26–33.

Dushenkov, S. (2003). Trends in phytoremediation of radionuclides. *Plant and Soil, 249*(1), 167–175.

Ebbs. S. D., Brady, D. J., Kochian, L. V. (1998). Role of uranium speciation in the uptake and the translocation of uranium by plants. *Journal of Experimental Botany, 49*(324), 1183–1190.

Environmental Protection Agency, EPA (1996). "Method 3050B: Acid Digestion of Sediments, Sludges, and Soils," Revision 2.

Gavrilescu, M., Pavel, L. V., Cretescu, I. (2009). Characterization and remediation of soils contaminated with uranium. *Journal of Hazardous Materials, 163*(2-3), 475-510.

Hu, N., Lang, T., Ding, D., Hu, J., Li, C., Zhang, H., & Li, G. (2019). Enhancement of repeated applications of chelates on phytoremediation of uranium contaminated soil by *Macleaya cordata*. *Journal of environmental radioactivity, 199*, 58-65.

Huang, J.W., Blaylock, M.J., Kapulnik, Y., Ensley, B.D. (1998). Phytoremediation of uranium-contaminated soils: Role of organic acids in triggering uranium hyperaccumulation in plants. *Environmental Science & Technology, 32*(13), 2004-2008.

Khan, A. G. (2020). In Situ Phytoremediation of Uranium Contaminated Soils. In Phytoremediation (p.p. 123-151). Springer, Cham.

Lesage, E., Meers, E., Vervaeke, P., Lamsal, S., Hopgood, M., Tack, F. M. G., Verloo, M. G. (2005). Enhanced Phytoextraction: II. Effect of EDTA and citric acid on heavy metal uptake by Helianthus annuus from a calcareous soil. *International Journal of Phytoremediation, 7*(2), 143–52.

Li, Z., Zhang, R., Zhang, H. (2018). Effects of plant growth regulators (DA-6 and 6-BA) and EDDS chelator on phytoextraction and detoxification of cadmium by *Amaranthus hybridus Linn.International Journal of Phytoremediation 20,* 1121-1128.

Malaviya, P., Singh, A. (2012). Phytoremediation strategies for remediation of uranium-contaminated environments: a review. *Critical Reviews in Environmental Science and Technology, 42*(24), 2575–2647.

Meng, F., Jin, D., Guo, K., Larson, L. S., Ballard, J. H., Chen, L., Arslan, Z., Yuan, G., White, J. R., Zhou, L., Ma, Y., Waggoner, C. A., Han, F. X. (2018). Influences of U Sources and Forms on Its Bioaccumulation in Indian Mustard and Sunflower. *Water, Air, & Soil Pollution, 229,*369.

Mihalík, J., Tlustoš, P., Szaková, J. (2010). Comparison of willow and sunflower for uranium phytoextraction induced by citric acid. *Journal of Radioanalytical and Nuclear Chemistry, 285*(2), 279–285.

Parra, R., Ulery, A. L., Elless, M. P., Blaylock, M. J. (2008). Transient phytoextraction agents: Establishing criteria for the use of chelants in phytoextraction of recalcitrant metals. International *Journal of Phytoremediation. 10*(5), 415–429.

Rostami, S., Azhdarpoor, A. (2019). The application of plant growth regulators to improve phytoremediation of contaminated soils: a review. *Chemosphere 220*, 818-827.

Schindler, M., Legrand, C. A., Hochella, Jr. M. F. (2015). Alteration, adsorption and nucleation processes on clay–water interfaces: Mechanisms for the retention of uranium by altered clay surfaces on the nanometer scale. *Geochimica et Cosmochimica Acta, 153,* 15–36.

Shahandeh, H., Hossner, L. R. (2002a). Enhancement of uranium phytoaccumulation from contaminated soils. *Soil Science, 167*(4), 269–280.

Shahandeh, H., Hossner, L. R. (2002b). Role of soil properties in phytoaccumulation of uranium. *Water, Air, & Soil Pollution, 141,* 165–80.

Vandenhove, H., Hees, M. V., Winckel, S. V. (2001). Feasibility of phytoextraction to clean up low-level uranium-contaminated soil. *International Journal of Phytoremediation, 3*(3), 301–320.

Wang, W. H., Luo, X. G., Liu, L., Zhang, Y., Zhao, H. Z. (2018). Ramie (Boehmerianivea)'s uranium bioconcentration and tolerance attributes. *Journal of Environmental Radioactivity, 184*, 152–157.

Yan, X., Luo, X. (2015). Radionuclides distribution, properties, and microbial diversity of soils in uranium mill tailings from southeastern China. *Journal of Environmental Radioactivity, 139*, 85–90.

Summary/Sažetak

Biljke posjeduju različite unutrašnje mehanizme koji su neophodni za akumulaciju i detoksikaciju kontaminanata iz tla a koji uključuju i radionuklide. Cilj ove studije bio je utvrditi biokoncentracijski faktor dvije brzo rastuće biljke, *Salvia offlicinalis* L. (kadulja) i *Ocimum basillicum* L. (bosiljak). Naime, biljke su kultivirane u pH neutralnim tlima i kontaminirane sa tri različite koncentracije urana (211-470 mg/ kg), a ispitana je i efikasnost limunske kiseline na unapređenje procesa fitoekstrakcije. Rezultati su pokazali da se biokoncentracijski faktor ne razlikuje značajno između dabranih biljnih vrsta (0.01-0.03). Naime, limunska kiselina je dodavana u dozama (50 mL, 30 mM) dok se nisu pojavili prvi efekti fitotoksičnosti urana, pri čemu je nakon četiri doze limunske kiseline biokoncentracijski faktor dostigao vrijednost od 0.05 za obje ispitivane biljke i izražen je povećani udio urana kod obje. Tako je pri istoj koncentraciji urana (470 mg/kg) u kontaminiranom tlu, udio urana u kadulji je porastao sa 6.03 na 21.28 mg/kg nakon dodatka limunske kiseline. Dobiveni rezultati potvrdili su efikasnost limunske kiseline u poboljšanju procesa fitoekstracije urana i nadalje sugeriraju da čak i biljke relativno male biomase mogu biti korisne u fitoremedijaciji ukoliko se primjeni odgovarajući tretman hemijskim sredstvima.

Glasnik hemičara i tehnologa Bosne i Hercegovine

Bulletin of the Chemists and Technologists of Bosnia and Herzegovina

2020

55

Print ISSN: 0367-4444
Online ISSN: 2232-7266

Original Scientific Article
DOI: https://doi.org/10.35666/ghtbh.2020.55.02
UDC: 547:577.1]633.886

7-12

Qualitative and quantitative determination of ligustilide as bioactive marker in apiaceous botanicals

Durić, K.*, Nikšić, H., Muratović, S., Gušić, I., Korić, E.

Faculty of Pharmacy, University of Sarajevo, Zmaja od Bosne 8, 71 000 Sarajevo, Bosnia and Herzegovina

Article info
Received: 17/03/2020
Accepted: 17/05/2020

Keywords:
ligustilide
Apiaceae
SFE
NMR

***Corresponding author:**
Kemal Durić
E-mail: kemal.duric@ffsa.unsa.ba
Phone: 00 387-61-213-307

Abstract: Variety of bioactivities has been associated with ligustilide present in root of *Angelica sinensis*, and predominantly used for the treatment of irregular menstrual cycles and premenstrual syndrome. Recent pharmacological studies showed that medicinal plants containing ligustilide, have anti-inflammatory effects and contribute to the improvement of cognitive functions, alleviate brain damage, inhibit tumor necrosis factor of some cell lines, and have nephron-protective effects and neuroprotective activity.

In this work, quantification of ligustilide using quantitative 1H NMR (qHNMR) in sealed tubes was performed. Four plant species were investigated: *A. sinensis*, *Ligusticum porteri*, *Ligusticum striatum*, and *Ligusticum sinense*. Modified supercritical CO_2 extraction of essential oil from root of four investigated species, was performed. qHNMR spectroscopy showed following percentage of ligustilide: *L. porteri* essential oil 3.74 (%); *L. sinense* essential oil 1.16 (%); *L. striatum* essential oil 6.61 (%) and *A. sinensis* essential oil 14.56 (%). The highest percentage of oil was obtained from the root of *L. porteri* but the highest percentage of ligustilide was obtained from *A. sinensis* essential oil.

INTRODUCTION

Phthalides such as the prototypical dihydro-phthalide (Z)-ligustilide (3-butylidene-4,5-dihydro-2-benzofuran-1-one) (Figure 1) are designated frequently as marker compounds of medicinal plants from the most prominent genera of the Apiaceae family, including Ligusticum and Angelica (Deng, 2005). Typically, depending on the phytochemical depth of the studies, ligustilide and its congeners are broadly associated with observed and ethno-botanically documented bioactivities of the plants and their preparations.

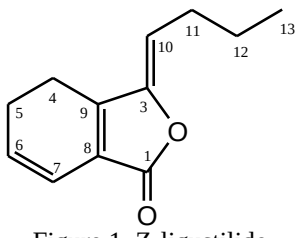

Figure 1. Z-ligustilide

Angelica sinensis is one of the 15 most commonly used Traditional Chinese Medicines (TCMs), predominantly in formulations for the treatment of irregular menstrual cycles and premenstrual syndrome (Wei, Zenq, Gu, *et al.*, 2016). Monograph of the root of *A. sinensis* was included in European pharmacopoeia as well. Recent pharmacological studies showed that medicinal plants containing ligustilide, have anti-inflammatory effects (Chung, Choi, and Seo, *et al*., 2012; Ma and Bai, 2013) improves the cognitive functions, alleviate brain damage (Feng, Lu, Wu, *et al.*, 2012), inhibit tumor necrosis factor of some cell lines (Shi, Xiao, Yin, *et al.*, 2015), and have nephron-protective effects and neuroprotective activity (Bunel, Antoine, Nortier, *et al.*, 2015; Wenxia, Yuzhi, Xiao, *et al.*, 2016**)**. The extraction techniques have focused on hexanes, pethroleum ether and other similar solvents as the initial strategy due to the relatively non polar characteristic of the majority of the phtalides. Furthermore, many phtalides are part of the essential oil composition of this botanicals and steam distillation was frequently used in order to obtaine this compounds (Cui, Fenq, and Hu, 2006). One of the

problem that occure during the extraction and isolation of this compounds, especially ligustilide, is due to its unstable nature.(Beck and Chou, 2007). This chemical and physical property makes preparations and conservation of the herbal products containing ligustilide very difficult. Many studies reported a considerable number of degradation products of ligustilide have been identified and their structures confirmed (Friesen, McAlpine, Chen, *et al.*, 2015; Schinkovitz, Pro, Main, *et al.*, 2008). One recent study on ligustilide stability, confirmed stability of this compound in essential oil and drug itself, but high instability of isolated compound was detected.(Quiroz-Garcia, Figueroa, Cogordan, *et al.*, 2005) The light strongly influenced the ligustilde transformation into its dimer – diligustilide, compond without any activity. The use of botanical dietary supplements with ligustilide as main component is increasingly popular, due to the number research studies that confirmed very important activities of this bio-active compounds. In paralel, with discovery of the herbal drugs containing ligustilide, the challenge is also to discover novel – non destructive analytical methods, that can easily enable quantitative determination of ligustilide, respecting its unstable nature (Zou, Chen, Zhao, *et al.*, 2018).

In this work, quantification of ligustilide in several botanicals, potentialy containing ligustilide, using quantitative ^{1}H NMR (qHNMR) was performed.

EXPERIMENTAL

Plant Material

Four ligustilide-rich species were investigated: *A. sinensis, L. porteri, L. striatum* and *L. sinense*. Plant materials, were purchased from Chinatown, Chicago, IL. The plants material were identified through a series of comparative macroscopic, organoleptic, and TLC analyses against an authentic *A. sinensis* voucher sample (BC440), *L. porter* voucher sample (BC576), *L. striatum* voucher sample (BC572) and *L. sinense* voucher sample (BC575), deposited at the UIC/NIH Center for Botanical Dietary Supplements Research, Chicago, IL. During experimental period the plant material was stored in a dry place, in the absence of light and in a cold location.

Supercritical Fluid Extraction

Extraction of essential oil from root of four investigated species, with modified supercritical CO_2 extraction method was performed. Supercritical fluid extraction (SFE) was performed on Speed SFE instrument, model 7070 (Applied Separation Inc. Allentown, PA), consisting of a column oven, air pressure regulator and 195 mm × 75 mm i.d. stainless steel column connected to a NESLAB RTE 7 refrigerated bath (Thermo Electron Corporation, Waltham, MA). Compressed air and CO_2 gases were purchased from Airgas Inc., Radnor, PA. The extraction column was filled with powdered plant material (69 g). Glass wool was added at each end of the column. As modifier, methanol was added at a concentration of 5% to the part of column where the CO_2 entered into the column. The extraction temperature was set to 50°C. Extraction was performed at 250 psi with static extract time of 30 min at a flow rate of 0.5 mL/min, 4 times for each sample. The SFE extract was then collected in glass vials and stored in a -20°C freezer.

Quantitative Nuclear Magnetic Resonance (qNMR) spectroscopy

Samples were dissolved in 600 μL of $CDCl_3$ using an analytical syringe (Valco Instruments, Baton Rouge, LA, USA). NMR experiments were performed on: Bruker Avance-360 MHz. The ^{1}H NMR experiments for stability evaluation and qHNMR quantification of ligustilide from the SFE extracts was performed using standard proton acquisition program ("zg 30"). Spectral width (SW) was 12 ppm, the shift of the center of the spectrum (O1P) was 7.9 ppm, acquisition time (AQ) was set to 2.77 s, receiver gain (RG) value was set to 512, and relaxation delay (D1) was 1 s. The spectra were processed and analyzed using MestReNova v9.0.1 (Mestrelab Research, Santiago de Compostela, Spain) software. A calibration curve was generated using dimethyl sulfone ($DMSO_2$, lot# BCBH9813V, Fluca analytical) as the external standard at concentrations ranging from 0.28 mM to 15.13 mM. The qHNMR data were processed as follows: baseline/Polynominal fit, zero-filling to 512 k prior to Fourier transformation of the FID and Zhu_Bax method, Lorenzian/Gaussian factor 0.25, manual peak by peak picking and integration.

RESULTS AND DISCUSSION

Most of phthalides, ligustilide included, are components of the essential oils, as they are mostly non-polar molecules. Extraction methods, conventionally used, includes steam distillation. One of the disadvantages of this method using water or water vapor is that essential oils undergo chemical alternation. Relatively high temperature could easily destroy sensitive compound and change oil composition and consequently its quality (Duric, Liu, Chen, *et al.*, 2019).

Therefore, it is very important that natural proportion of the component in essential oil is maintained during the extraction from plant material by any procedure (Răileanu, Todan, Voicescu, *et al.*, 2013; Turek, and Stintzing, 2013).

In this work essential oils from four different plant species were obtained by supercritical CO_2 fluid extraction. Modification of supercritical CO_2 method includes addition of modifier MeOH (5%), into column with plant material, in order to enhance the solubility of lipophilic components. Static extraction time from 20 minutes was prolonged to 30 minutes per every extraction. Flow rate from 2.0 mL/min was decreased to 0.5 mL/min., which aims to extend the contact of the solvent and plant material (Table 1).

Table 1. Comparison of extraction conditions Between Standard and Modified Method

Extraction conditions	Standard	Modified
Extract temperature	50°C	50°C
Vessel temperature	120°C	120°C
Pressure	250 psi	250 psi
Static extract time	20 min	30 min
Flow rate	2 mL/min	0.5 mL/min
Modifier	no	5% MeOH

After extraction with CO_2 was performed, four essential oils of different shades of pale yellow color were obtained. The yield of essential oils, ranged from 0.35 g/100g to 7.3 g/100g of dry plant material (Figure 2). Prior to analyses of the Z-ligustilide content in the essential oils, obtained essential oils were stored at -20°C.

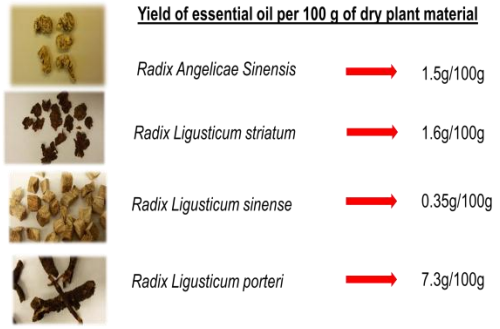

Figure 2. Yield of essential oil obtained by SFE extraction using modified method.

Extraction with supercritical fluid allows to obtain an essential oil at relatively low temperature, 50°C in our case, which could explain better yield of the oil itself.
Since Z-ligustilide was a compound of interest in this study, after essential oils were obtained, percentage of Z-ligustilide were quantified using qHNMR (Gödecke, Napolitano, Rodriguez Brasco, *et al.*, 2013). Quantification of Z-ligustilide was done thanks to the characteristic signal of this compound doublet of triplet at δ 6.286 (1H, H-7) and calibration with dimethyl sulfone ($DMSO_2$) as external standard (EC qHNMR) (Pauli, Chen, Simmler, *et al.*, 2014; Pauli, Gödecke, Jaki, *et al.*, 2012).

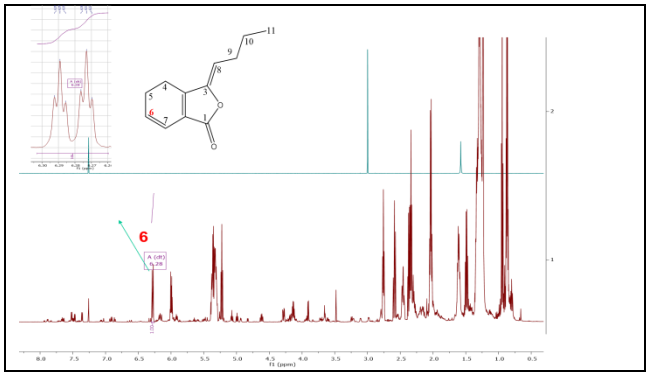

Figure 3. HNMR spectra of essential oil of *Angelica sinensis* with characteristic peak at δ 6.286 (1H, H-7).

Although the essential oil has a complex structure and consequently overlapped NMR spectra, the characteristic signal was possible to identified (Simmler, Napolitano, McAlpine, *et al.*, 2014). Figure 3 shows the HNMR spectra of essential oil of *A. sinensis*.

Quantitative analysis was performed using absolute quantification (100% method). This method allows the determination of the mass of a compound with known structure (Z-ligustilide in our case) in an accurately weighed sample. It involves the use of a calibrant of known exact weight and purity. When using an external calibrant (EC), the general calculation of purity (P) was done according to following formula:

$$P_{analyte} = \frac{I_{analyte} \times N_{EC} \times M_{analyte} \times W_{EC} \times P_{EC}}{I_{EC} \times N_{analyte} \times M_{EC} \times W_{sample}}$$

where, P is the purity of the analyte (in %), I is the absolute integral value, N is the number of protons in the integrated signal, M is the molar mass, W is the gravimetric weight (in mg), EC is the external calibrant.
The calculated percentage of ligustilide in four investigated essential oils were presented in Figure 4.

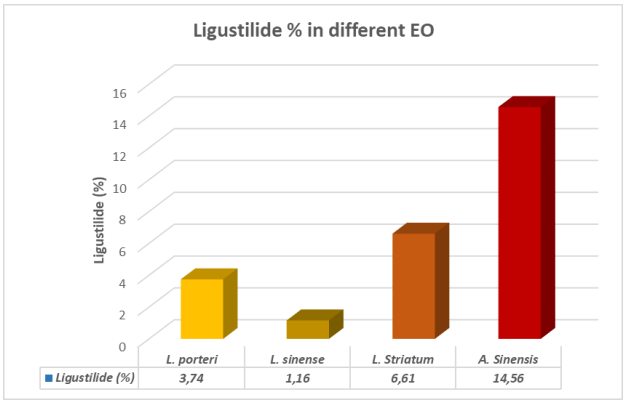

Figure 4. Ligustilide content (%) in different essential oils obtained from plant species belonging to Apiaceae family

Quantification for each oil was made in triplicate. Previous work with non modified method of supercritical CO_2 extraction indicate 10% of ligustilide in essential oil of *A. sinensis* (Yi, Liang, Wu, *et al.*, 2009; Zhou, and Li, 2001). This shows that modified method is much more efficient because it gives a higher yield of ligustilide. The highest amount of essential oil was found in plant species *L. porteri* (7.3 g of essential oil/100 g of dry plant material) but the essential oil with the highest percentage of ligustilide was oil obtained from *A. Sinensis* (14.56%). Calculating the quantity of ligustilide per 100 g of plant material it comes out that *L. porteri* is the species with the highest amount of ligustilide with 0,27g of ligustilide/100g of plant material, followed by *A. sinensis* 0,21g/100g, *L. striatum* 0,11g/100g and L. sinense 0,004 g/100 g. Although *L. porteri* has been used for treatment of wild range of

illness in ethno medicine, there is scarce scientific data about its activity and pharmaceutical usage (Beck and Chou, 2007). The results about ligustilide content in *L. porteri*, obtained in this research, open new possibilities for use of this plant species as a source of ligustilide.

CONCLUSIONS

Although plenty of pharmaceutical effects of *Z*-ligustilide have been reported, study on the activities of *Z*-ligustilide is still inadequate. The main reason is the instability of *Z*-ligustilide, and its easily transformation into other degradation products by oxidation, isomerization, and dimerization at an elevated temperature. Different extraction techniques involve laborious operations and consume large amounts of organic solvents. More over these techniques used a high temperature which is unfavorable to ligustilide. The extraction of essential oils using supercritical fluids present an alternative to conventional methods, and it is much faster, more simple and efficient. This article summarized research outcomes involving optimization of parameters of supercritical extraction for maximum recovery of analytes. The SFE method and conditions applied in this work prove to be more efficient in obtaining essential oil with major percent of Z-ligustilide. The environmental friendliness of this technique with non toxic carbon dioxide as main solvent, represent u huge advantage towards organic solvents. qHNMR technique and method of quantification using external standard, allowed to quantified this compound in the essential oil and herbal preparations. Nondestructive nature of NMR, prove to be optimal analytical method for determination of ligustilde in the essential oil sample. Also, this method could be used for the tracking of the Z-ligustilide degradation in different herbal formulations. This is very important from the point of view of the instability of this molecule, especially with regard to the fact that it is a bioactive marker for many apiaceous botanicals.

ACKNOWLEDGMENTS

This research was supported by Dr. Pauli research group at the UIC College of Pharmacy, Chicago, Illinois, USA. K.D. would like to acknowledge a Fulbright fellowship (Grantee ID: 68150333) which made it possible for him to pursue research activities in the USA.

REFERENCES

Beck, J. J. Chou, S. C. (2007). The Structural Diversity of Phthalides from the Apiaceae. *Journal of Natural Product, 70 (5)*, 891-900.

Bunel, V., Antoine, M. H., Nortier, J., Duez, P., Stevigny, C. (2015). Nephroprotective effects of ferulic acid, Z-ligustilide and E-ligustilide isolated from Angelica sinensis against cisplatin toxicity in vitro. *Toxicology in Vitro, 29 (3)*, 458-467.

Chung, J. W., Choi, R. J., Seo, E. K., Nam, J. W., Dong, M. S., Shin E. M., Guo L. Y., Kim, Y. S. (2012). Anti-inflammatory effects of (Z)-ligustilide through suppression of mitogen-activated protein kinases and nuclear factor-κB activation pathways. *Archives of Pharmcal Research, 35 (4)*, 723-732.

Cui, F., Fenq, L., Hu, J. (2006). Factors affecting stability of *Z*-ligustilide in the volatile oil of *radix Angelicae sinensis* and *Ligusticum chuanxiong* and its stability prediction. *Drug Development and Industrial Pharm*acy, *32*, 747-755.

Deng, S. Phytochemical Investigation of Bioactive Constituents from *Angelica sinensis*. Ph.D. Dissertation, University of Illinois at Chicago, Chicago, IL, 2005.

Duric, K., Liu, Y., Chen S. N., Lankin, D.C., Nikolic, D., McAlpine, J. B., Friesen, J. B., Pauli, G. F. (2019). Studying Mass Balance and the Stability of (*Z*)-Ligustilide from *Angelica sinensis* Helps to Bridge a Botanical Instability–Bioactivity Chasm. *Journal of Natural Products, 82(9), 2400-2408*

Feng, Z., Lu, Y., Wu, X., Zhao, P., Li, J., Peng, B., Qian, Z., Zhu, L. (2012). Ligustilide alleviates brain damage and improves cognitive function in rats of chronic cerebral hypoperfusion. *Journal of Ethnopharmacology, 144 (2)*, 313-321.

Friesen, J. B., McAlpine, J. B., Chen, S. N., Pauli, G. F. (2015). Countercurrent Separation of Natural Products: An Update. *Journal of Natural Product, 78 (7)*, 1765-1796.

Gödecke, T., Yao, P., Napolitano, J. G., Nikolic, D., Dietz, B. M., Bolton, J. L., van Breemen, R. B., Farnsworth, N. R., Chen, S. N., Lankin, D. C., Pauli, G. F. (2012). Integrated standardization concept for Angelica botanicals using quantitative NMR. *Fitoterapia, 83 (1)*, 18-32.

Gödecke, T., Napolitano, J. G., Rodriguez Brasco, M. F., Chen, S. N., Jaki, B. U., Lankin, D., Pauli**,** G. F. (2013). Validation of a Generic qHNMR Method for Natural Products Analysis. *Phytochemical Analysis, 24*, 581-597.

Ma, Z., Bai, L. (2013). Anti-inflammatory effects of Z-ligustilide nanoemulsion. *Inflammation, 36 (2)*, 294-299.

Pauli, G. F., Chen, S. N., Simmler, S., Lankin, D. C., Gödecke, T., Jaki, B. U., Friesen, J. B., McAlpine, J. B., Napolitano, J. G. (2014). Importance of purity evaluation and the potential of quantitative ^{1}H NMR as a purity assay. *Journal of Medicinal Chemistry, 57*, 9220-9231.

Pauli, G. F., Gödecke, T., Jaki, B. U., Lankin, D. C. (2012). Quantitative ^{1}H NMR. Development and Potential of an Analytical Method: An Update**.** *Journal of Natural Product, 75 (4)*, 834-851.

Quiroz-Garcia, B., Figueroa, R., Cogordan, J.A., Delgado, G.(2005).Photocyclodimers from Z-ligustilide. Experimental results and FMO analysis. *Tetrahedron Letters, 46*, 3003-3006.

Răileanu, M., Todan, L., Voicescu, M., Ciuculescu, C., Maganu, M. (2013). A way for improving the stability of the essential oils in an environmental friendly formulation. *Materials Science & Engineering C-Materials for Biological Applications*, *33 (6)*, 3281-3288.

Schinkovitz, A., Pro, S. M., Main, M., Chen, S. N., Jaki, B. U., Lankin, D. C., Pauli, G. F. (2008). Dynamic nature of the ligustilide complex. *Journal of Natural Product*, *71 (9)*, 1604-1611.

Shi, Y. S., Xiao, L., Yin, Y., Wei, L. (2015). Ligustilide inhibits tumour necrosis factor-alpha-induced autophagy during C_2C_{12} cells differentiation. *Biomedicine& Pharmacothererapy*, *69*, 42-46.

Simmler, C., Napolitano, J. G., McAlpine, J. B., Chen, S. N., Pauli, G. F. (2014). Universal quantitative NMR analysis of complex natural samples. *Current Opinion in Biotechnology*, *25*, 51-59.

Turek, C., Stintzing, F. C. (2013). Stability of essential oils: A review. *Comprehensive Reviews in Food Science and Food Safety, 12, 40-53*

Wei, W. Zenq, R. Gu, C. M. Qu, Y. Huang L. F. (2016). *Angelica sinensis* in China-A review of botanical profile, ethnopharmacology, phytochemistry and chemical analysis *Journal of Ethnopharmacology*, *190*, 116-141.

Wenxia, G., Yuzhi, Z., Xiao, L., Xiaoxia, G., Junsheng, T., Xuemei, Q., Guanhua, D. (2016). Neuroprotective and cytotoxic phthalides from *Angelicae sinensis* radix. *Molecules, 21 (5)*, 549.

Yi, L., Liang, Y., Wu, H. Yuan, D. (2009). The analysis of radix Angelicae sinensis (Danggui). *Journal of Chromatography A, 1216 (11)*, 1991-2001.

Zhou, C., Li, X. H. (2001). Studies on the stability of ligustilide with solvent effect. *Acta Pharmaceutica Sinica, 36 (10)*, 793-795**.**

Zou, J., Chen, G. D., Zhao, H., Huang, Y., Luo, X., Xu, W., He, R. R., Hu, D., Yao, X. S., Gao, H. (2018). Triligustilides A and B: two pairs of phthalide trimers from *Angelica sinensis* with a complex polycyclic skeleton and their activities. *Organic Letters*, *20 (3)*, 884-887.

Summary/Sažetak

Ligustilid je označen kao glavna aktivna komponenta biljne vrstie *Angelica sinensis*, koja se prevashodno koristi kod neredovnog menstrualnog ciklusa i predmenstrualnog sindroma. Najnovija farmakološka ispitivanja potvrđuju da ljekovite biljke koje sadrže ligustilid, imaju protuupalno djelovanje, poboljšavaju kognitivne funkcije, ublažavaju oštećenje mozga nakon hipoksije, inhibiraju faktor nekroze tumora određenih ćelijskih linija, imaju nefron-zaštitne učinke i neuroprotektivnu aktivnost. U ovom radu provedeno je kvantitativno određivanje ligustilida, pomoću kvanti 1HNMR metode. Ispitane su četiri vrste biljaka: *Angelica sinensis, Ligusticum porteri, Ligusticum striatum* i *Ligusticum sinense*. Ekstrakcija eteričnog ulja iz korijena četiri ispitivane vrste, provedena je modificiranom metodom sa superkritičnim CO_2. qHNMR analiza pokazala je sljedeći postotak ligustilida: eterično ulje *L. porteri* 3,74 (%); eterično ulje *L. sinense* 1,16 (%); eterično ulje *L. striatum* 6,61 (%) i eterično ulje *A. sinensis* 14,56 (%). Najveći postotak ulja dobiven je iz korijena *L. porteri*, ali najveći postotak ligustilida sadržavalo je eterično ulje *A. sinensis*.

Glasnik hemičara i tehnologa Bosne i Hercegovine

Bulletin of the Chemists and Technologists of Bosnia and Herzegovina

2020

55

13-18

Print ISSN: 0367-4444
Online ISSN: 2232-7266

Original Scientific Article
DOI: https://doi.org/10.35666/ghtbh.2020.55.03
UDC: [546.72+547.576]:543.544.164

Synthesis and characterization of Fe(III) complex with thiosemicarbazide-based ligand

Ljubijankić N.[a] , Galijašević S.[b*]

[a]*Faculty of Science, Department of Chemistry, Zmaja od Bosne 33-35, Sarajevo, Bosnia and Herzegovina*
[b]*School of Science and Technology, Sarajevo Medical School, Department of Medical Chemistry and Biochemistry, Hrasnička cesta 3b, Sarajevo, Bosnia and Herzegovina*

Article info
Received: 28/08/2020
Accepted: 15/09/2020

Keywords:
Salicylaldehyde thiosemicarbazone
iron-thiosemicarbazone complex
antioxidant activity
FT-IR

***Corresponding author:**
Semira Galijašević
E-mail: semira.galijasevic@ssst.edu.ba
Phone: 00 387-62-410-878

Abstract: Complex iron(III) salicylaldehyde thiosemicarbazone with a formula $Na[Fe(STSC)_2]$ have been synthesized. Ligand, salicylaldehyde thiosemicarbazone (SCT) was prepared through the condensation reaction of salycilaldehide with thiosemicarbazide. $Na[Fe(STSC)_2]$ has been synthesized by reacting $FeCl_3$ with thiosemicarbazide based ligand bearing ONS donor atoms. Complex has been formulated and characterized by mass spectrometry, infrared and UV/visible spectroscopy. The facts showed the formation of a complex in metal:ligand stoichiometric ratio 1:2. The ligand is coordinated as an ONS tridentate dianion *via* oxygen atom after the deprotonation of the phenolic OH-group, azomethine nitrogen and sulphur in thiol form of the deprotonated thiosemicarbazide residue. Antioxidant activity was determined, where ligand showed significant activity, while complex, at low concentration, exhibited almost no activity.

INTRODUCTION

Thiosemicarbazones have been a focus of a research for a long time due to its biological activities. These compounds and its derivatives showed antiviral, antibacterial and antineoplastic effects with different levels of activity. Moreover, the complexes of thiosemicarbazone with metals showed significant biological activity especially due to the changed lipophilicity that allows better deposition in the cell. This is due to their redox properties and lately discovered mechanism of action that involves the Fenton chemistry in the cases of an iron-thiosemicarbazone complexes. As a result, the production of free radicals, especially reactive oxygen species (ROS) is increased that in turn leads to the antiproliferative effect. In addition, if thiosemicarbazone are used alone as an active substances, they can sequester iron ions from the cell by chelation mechanism that will cause the inhibition of compounds with an iron in the structure such as heme containing enzymes of iron-protein compounds.

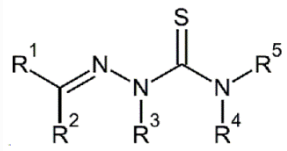

Figure 1.General structure of thiosemicarbazones where X represents sulfur atom while R_1, R_2 and R_3 represents alkyl or aryl groups.

Anti-tumor activity of thiosemicarbazone complexes have been explained by mechanism that involves depletion of iron from the tumor cells first and formation of Fe(III) complex. Due to the number of cellular reductant and oxidant, redox turnover between Fe(III) and Fe(II) complexes occurs. During this process, in the case of iron complexes, Fenton reaction produces ROS that are damaging tumor DNA bases resulting in cytotoxicity and destruction of tumor cells (Alcaraz, Muñiz, Cavia, et al. 2020).

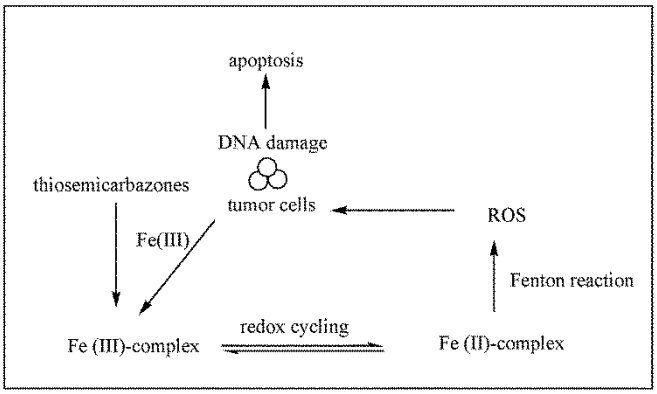

Figure 2. Cytotoxicity mechanism

Besides iron complexes showing antitumor activities, some copper(II) complexes of 3-etoxy-2-oxobutyraledehyde-bis(thiosemicarbazone) showed a strong antitumor activity in animal studies. Further studies proved that variation in a ligand structure of these complexes significantly affected the cytotoxic effect. Wide spectrum of anti-microbial effects was detected for the different thiosemicarbazone with complexes with metals. Generally, complexes showed strong activity against *Staphylococcus aureus*, *Neisseria meningitidis*, while poor activity against the gram-negative bacilli (Dobek, Klayman, Dickson et al. 1989). In these cases, mechanism of the action of the complexes was explained by electron transfer and free radical activity against microbes. Other potent effects that thiosemicarbazone includes are anticonvulsant activity and antiviral activity either as a ligand or in the complex with a various metals. A recent study found that pyridyl thiosemicarbazones are highly potent agents for the treatment of malaria. Generally, standard compounds used for the treatment such as chloroquine showed the interaction with parasitic heme resulting in a pH-dependent decomposition of the heme (Chou, Chevli Fitch, 1980; Slater, Cerami, 1992; Dorn, Vippagunta, Matile et al.,1998). Thiosemicarbazones derived from phenolic aldehydes showed similar anti-malarial activity, based on its ability to chelate iron. Clearly, the synthesis and the investigation of the thiosemicarbazone complexes with metals, especially with iron justify the research in order to detect exact mechanism of it activity and potency in biological systems. In this study, we synthesized and characterized iron(III) salicylaldehyde thiosemicarbazone complex and tested their antioxidant activity.

EXPERIMENTAL

Material

All chemical used in the study were obtained from Sigma Aldrich and Merck. Commercial reagents of analytical reagent grade were used without further purifications. Solvents used in the synthesis of the ligand and their complex were distilled before use.

Methods

ESI ToF MS were obtained on 6210 Time-of-Flight LC/MS instrument (Agilent Technologies, California, USA) connected with Agilent 1200 Series HPLC instrument (Agilent Technologies, Waldbronn, Germany), Instrument consisted of degasser, binary pump, autosampler, column compartment with ZDV (zero dead volume) cell and diode-array detectors (DAD). The mobile phase consists of 0.2% formic acid in water (v/v) (A) and acetonitrile (B) in a 1:1 ratio. Flow mobile phase is 0.20 mL/min, column compartment temperature 25°C, and injection volume of samples c≈1 mg/mL 5 μL. Peak spectral data were stored in the range 190-450 nm. Mass spectra were recorded in the range of 100-2000 m/z in negative ESI ionization mode (capillary voltage 4000 V, fragment voltage 140 V, skimmer voltage 60V, OCT RF voltage 250V); spray gas (nitrogen): pressure 45 psi, temperature 350°C, flow 12 L/min.

FTIR spectra were recorded using KBr pellets on a Perkin Elmer spectrum BX FTIR System in the region 4000-400 cm^{-1}.

The electronic absorption spectra from 200 nm to 7000 nm were recorded with Thermo Scientific Multiscan Go using quartz cuvettes with a 1 cm path length.

Antioxidant capacity of the ligand and a complex was tested by e-BQC lab instrument (bioquochem, CEEI Parque Tecnológico de Asturiasis) based on a redox potential of the tested compounds and its comparison with antioxidant activity of ascorbic acid. Measurements are expressed in charge units- micro-Coulombs (μC). To compare the results (μC) to antioxidant capacity units of Vitamin C Antioxidant Capacity Equivalents (CEAC) are used. Briefly, calibration curve with a standard solution of ascorbic acid diluted in a standard buffer solution was used to measure charge values (μC). Regression line was used to obtain the equation: Charge value (μC)=a Concentration (μM) + b where measured charge values of a tested solutions were used and converted to concentrations of the tested samples that have equivalent antioxidant capacity as a model antioxidant (CEAC) (Rey, Gómez, Muñoz-Cimadevilla et al, 2018). Ligand and complex were dissolved in a dichloromethane and then diluted with the 150 mM phosphate buffer pH 7.4 in order to minimize the effect of the organic solvent on e-BQC measuring strips.

Synthesis of ligand salicylaldehyde thiosemicarbazone

The amount of 0.911 g thiosemicarbazide (0.01 mol) was dissolved in 75 mL of warmed distilled water and volume of 1.044 mL salicylaldehyde (0.01 mol) was added to the solution. The reaction mixture was refluxed for 5 hours at 55-60°C. Afterwards, solution was cooled on ice bath and the crystals of white salicylaldehyde thiosemicarbazone were collected by filtration, dried by vacuum pump and recrystallized from ethanol with 75% yield (Archana, Ezhilarasi, 2012). Ligand is insoluble in water and benzene, soluble in dimethylformamide, dimethyl sulfoxide and dichloromethane.

White solid; Yield: (75%). M.p. 250°C. FT-IR(KBr): ν, cm^{-1} 1263 (C-O), 1616 (C=N),777(C=S), UV-Vis (DMF): λ_{max}, nm 234, 309, 334.

Synthesis of iron(III) salicylaldehyde thiosemicarbazone, Na[Fe(STSC)$_2$]

The amount of 0.135 g of iron (III) chloride ($FeCl_3.6H_2O$) (0.0005 mol) was dissolved in 15 mL of slightly warmed methanol and mixed with 0.204 g (0.0015 mol) of sodium acetate three hydrate ($NaOAc \cdot 3H_2O$). After cooling to room temperature, the solution was filtered and ligand, salicylaldehyde thiosemicarbazone (0.195 g, 0.001 mol) was added. The mixture was gently heated at 45-50 °C for about 30 minutes with continuous stirring. After the mixture was cooled to a room temperature, separation of the solid was observed. The mixture was left at room temperature over the next 24 hours resulting in complete precipitation of a black solid. Subsequently, the obtained complex was filtered, the crystals washed with methanol and ether and dried in a vacuum desiccators (Semanti, Rama, Falgun et al., 2010; Sulekh, Lokesh, 2005).

Insoluble in water, benzene, soluble in dimethylformamide, dimethyl sulfoxide and dichloromethane.

Black solid; Yield: (71%). M.p. 227°C. FT-IR (KBr): ν, cm^{-1} 11304 (C-O), 1603 (C=N), 737 (C-S), 590 (Fe-N), 457 (Fe-O), 427 (Fe-S); UV-Vis (DMF): λ_{max}, nm 238, 308, 337. ESI ToF m/z =441.99746 $[M+ H]^+$

RESULTS AND DISCUSSION

Ligand salicylaldehyde thiosemicarbazone and a complex iron(III) salicylaldehyde thiosemicarbazone were synthesized from the starting compound thiosemicarbazide by modified synthesis procedures. Complex was synthesizes in the presence of sodium acetate three hydrate with the addition of $FeCl_3 \cdot 6H_2O$ (Figures 3 and 4).

Obtained ligand and a complex were insoluble in the water, benzene or chloroform, but soluble in the dimethylformamide, dimethylsulfoxide and dichloromethane. Synthesized compounds were characterized by UV/Visible spectroscopy and FT-IR. Mass spectroscopy confirming the presence of a newly formed complex.

ESI ToF mass spectrometry confirmed existence of $[C_{16}H_{14}N_6O_2S_2Fe]^-$, ion with m/z values at 441.99746 amu. Spectra showed a series of peaks at 199.8; 194.039; 318.901; 640.8082 that are corresponding to the various fragments (Figure 5).

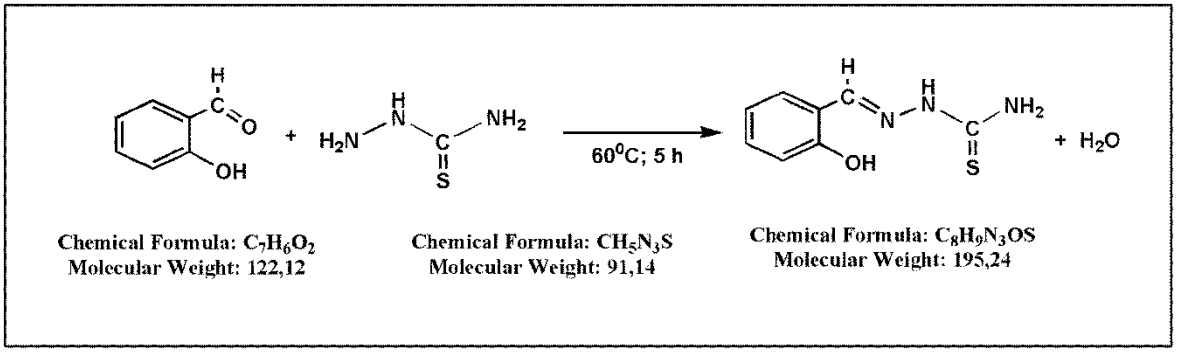

Figure 3. Ligand synthesis, thiosemicarbazone salicylaldehyde (STSC)

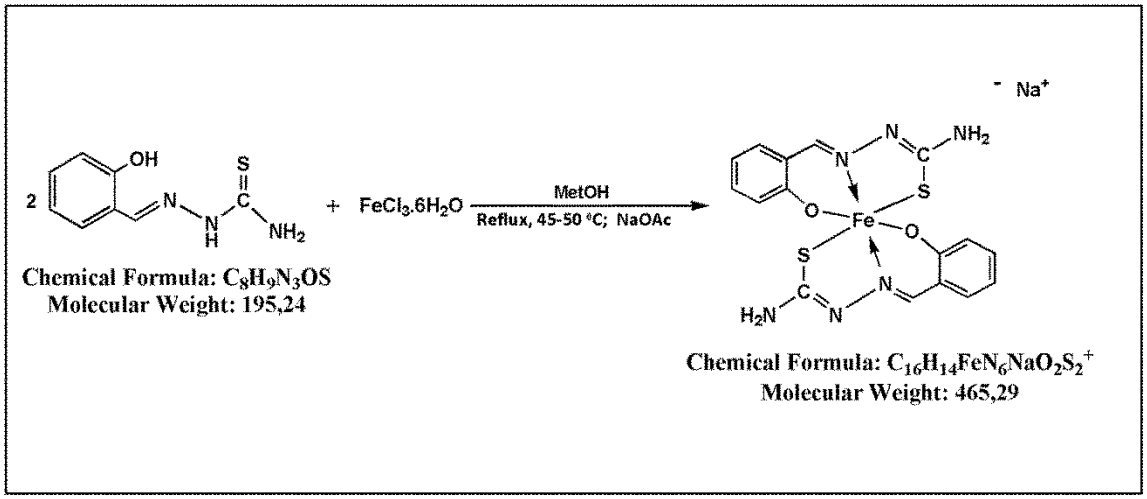

Figure 4. Synthesis of iron(III) complex with salicylaldehyde thiosemicarbazone, Na[Fe(STSC)$_2$]

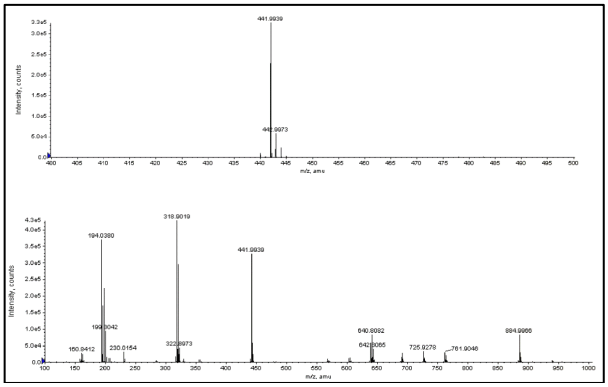

Figure 5. Mass spectrum of Na [Fe (STSC) 2]

Table 1. Calculated and experimental mass spectra data for the molecular ion

Molecular ion	$C_{16}H_{14}N_6O_2S_2Fe^-$
Theoretical mass	441.99746
Experimental mass	441.99775
Error in mass /mDa	0.29458
Error in mass/ppm	0.67

IR spectra were recorded for the ligand and a complex in the region of 2300 to 400 cm^{-1}, analyzed and the assignment of the detected frequencies have been compared with the literature values for the specific group vibrations. The Table 2 shows the assigned values for the ligand and the complex.

Table 2. FT-IR data for the ligand and complex (2300 to 400 cm^{-1})

Peak assignment	**ν(C=N) cm^{-1}**	**ν(C-O) cm^{-1}**	**ν(C=S) cm^{-1}**	**ν(C-S) cm^{-1}**	***ν*(Fe–N) cm^{-1}**	***ν*(Fe–O) cm^{-1}**	***ν*(Fe–S) cm^{-1}**
STSC	1616	1263	777	-	-	-	-
Na[Fe(STSC)$_2$]	1603	1304	-	737	590	457	427

STSC-salicylaldehyde thiosemicarbazone, Na[Fe(STSC)2]-iron (III) salicylaldehyde thiosemicarbazone

The ligand is coordinated to iron center as a ONS tridentate dianion *via* oxygen atom after the deprotonation of the phenolic OH-group, azomethine nitrogen and sulphur in thiol form of the deprotonated thiosemicarbazide. This was confirmed by IR spectra: shift of azomethine stretching to lower frequency, shift of C-O(H) vibration to higher frequency and disappearance of the vibration of C=S double bond in the spectra of the complex (El-Bahnasawy et al., 2014).

In order to analyze the way of ligand coordination to the metal, the most significant infrared spectral frequencies for the metal complex are compared with the frequencies of the free ligand. A band observed at 1616 cm^{-1} attributed to the azomethine C=N stretching frequency of the free ligand where shifted to lower frequency in the spectra of the complex at 1603 cm^{-1} indicating the coordination through N atom. Deprotonated phenolic oxygen – strong absorption band in spectra of ligand positioned at 1263 cm^{-1} after coordination is shifted to 1304 cm^{-1} (Baiu et al., 2009), which corresponds to forming of weaker C-O(Fe) bond comparing to C-O(H) and confirms coordination of ligand to Fe(III) through deprotonated phenolic oxygen. Also, in the IR spectra of ligand, the characteristic vibration of the (OH) band is observed at 3444 cm^{-1}. The absence of this band in the IR spectra of the complex indicates the coordination *via* the phenolic oxygen (Vojinović- Ješić et al., 2011). The ligand showed band at 777 cm^{-1} for ligand for the vibration of the C=S bond (Wiles et al., 1967; Thangadurai et al., 2001). The C=S band was disappeared in the complex (Al-Amiery et al., 2011) and a new band, C–S appeared at 737 cm^{-1}.

This confirms that the other coordination site to iron is through thiolate sulphur (Sampath et al., 2016). The new bands at 590, 457 and 427 cm^{-1} are attributed to Fe–N, Fe–O and Fe–S bonds, respectively (El-Bahnasawy et al., 2014) (Figure 6).

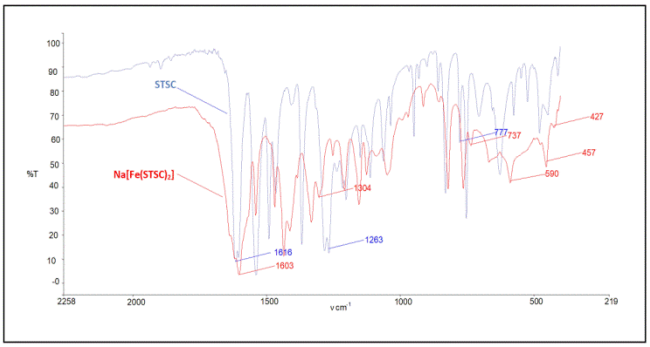

Figure 6. FT-IR spectra of ligand (STSC, blue line) and complex (Na[Fe(STSC)$_2$, red line)

UV/Visible spectra were recorded for the ligand and the complex in the range from 220 to 700 nm. Ligand showed maximum peak with higher intensity at 241 nm, peak at 291nm and one peak at 345 nm with a lower intensity. The spectra of the ligand showed characteristic π→π* and n→π bands due to the substituted benzene group. UV/Vis spectra of the complex showed peaks at 241 nm and 291 nm, and a shoulder at 345 nm due to the complexation.

The d-d transition in this type of complexes usually showed above 500 nm but in this case, probably to the weak transition was not clearly detected (Figure 7).

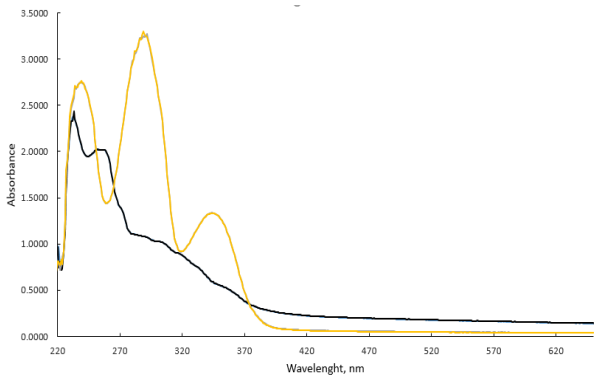

Figure 7. UV/Visible spectra of ligand (yellow line) and a complex (black line)

A number of thiosemicarbazide derivatives have been tested for antioxidant activity and attempts have been made to correlate specific structural features with antioxidant ability of the synthesized compounds based on the thiosemicarbazide structure (Ghosh, Misra, Bhatia et al, 2009). The amine group in thiosemicarbazone moiety significantly contributes to the antioxidant activity of the compound. In addition, phenolic hydroxyl group with its electron donation ability is involved in the increased antioxidant activity. However, complexation with the metal decreases its antioxidant ability due to its involvement into metal coordination process.

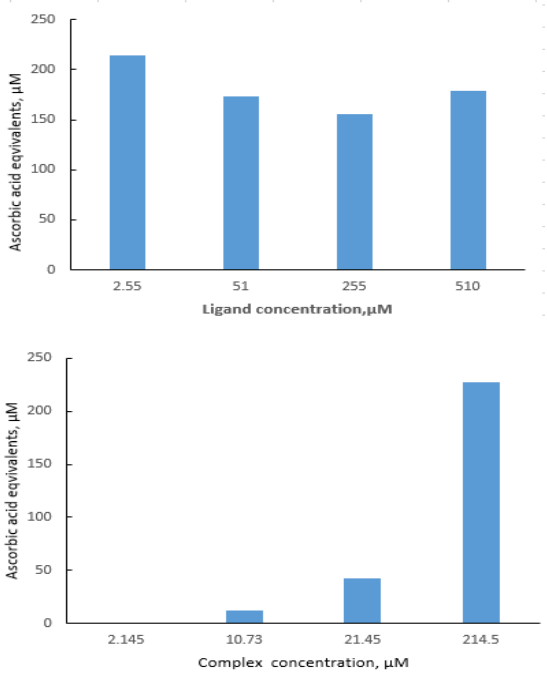

Figure 8. Total antioxidant capacity of a salicylaldehyde thiosemicarbazone (A) and iron(III) salicylaldehyde thiosemicarbazone (B) expressed in ascorbic acid equivalents, µM

Salicylaldehyde thiosemicarbazone showed substantial antioxidant capacity that was not dependent on the concentration of the ligand (Figure 8). Iron(III) salicylaldehyde thiosemicarbazone antioxidant activity was almost negligent at the lower micromolar concentration. Only at a high concentration of the complex (214.5 µM) a high antioxidant activity was observed that can be attributed only to free amine groups in the structure.

CONCLUSIONS

We synthesized and characterized salicylaldehyde thiosemicarbazone ligand and its complex, iron (III) salicylaldehyde thiosemicarbazone. Structures were confirmed by mass spectra, and FT-IR methods and UV/Visible spectra were recorded with characteristic maximum wavelengths. Antioxidant activities that are expected for this type of compounds were measured, where ligand showed a high activity regardless of the tested concentration, while a complex showed significant activity only at the higher concentrations. Further studies should be done in order to correlate specific structural features with antioxidant activity and modulation of it that would allow formation of the stable complex, and at the same time, formation of the stable complex.

REFERENCES

Al-Amiery A. A., Kadhum A.A.H., Abdulreazak H. and Mohamad A.B. (2012). Antifugal and Antioxidant Activites of Pyrrolidone Thiosemicarbazone Complexes. *Bioinorganic Chemistry and Applications*, 1-6.

Alcaraz R, Muñiz P, Cavia M, et al. (2020) Thiosemicarbazone-metal complexes exhibiting cytotoxicity in colon cancer cell lines through oxidative stress. *J Inorg Biochem.;206:110993.*

Archana S., Ezhilarasi Rosaline J.(2012) Synthesis Characterization and Application of Salicylaldehyde Thiosemicarbazone and Its Metal Complexes, *International Journal of Research in Chemistry and Environment*, Vol. 2 Issue 4;130-148

Baiu S.H., El-Ajaily M.M. and El-Barasi. (2009). Antibacterial Activity of Schiff Base Chelates of Divalent Metal Ions. *Asian Journal of Chemistry*. 21(1), 5-10

Chou, A.C., Chevli, R, Fitch C.D. (1980) Ferriprotoporphyrin IX fulfills the criteria for identification as the chloroquine receptor of malaria parasites. *Biochemistry*, 19: 1543–9.

Dobek A.S.; Klayman D.L.; Dickson Jr., E.T.; Scovill J.P.; Tramont E.C.(1980)Inhibition of clinically significant bacterial organisms in vitro by 2-acetylpyridine thiosemicarbazones. *Antimicrob. Agents* Chemother. 18, 27

Dorn, A., Vippagunta, S.R, Matile, H *et al.* (1998) An assessment of drug–haematin binding as a mechanism for inhibition of haematinpolymerisation by quinoline anti-malarials. *Biochem Pharmacol* 1998; 55: 727–36.)

El-Bahnasawy R. M., Sharaf El-Deen L. M., El-Table A.S., Wahba M. A. and El-Monsef.A. (2014). Electrical Conductivity Of Salicylaldehyde Thiosemicarbazone and its Pd(II), Cu(II) and Ru(III) Complexes. *Eur. Chem. Bull*, 3(5), 441-446.

Ghosh,S., Misra, AK., Bhatia,G., Khan,MM., Khanna, AK. (2009)Syntheses and evaluation of glucosyl aryl thiosemicarbazide and glucosyl thiosemicarbazone derivatives as antioxidant and anti-dyslipidemic agents.*Bioorganic & Medicinal Chemistry Letters* 19 (2), 386-389.

Sapath K. and Jayabalakrishnan C. (2016). Ruthenium(III) Thiosemicarbazone Complexes Synthesis, Characterization, DNA Binding, Antibacterial, In vitro Anticancer and Antioxidant Studies. *Journal of Engineerng Chemistry and Fuel*, 1(1), 40-53.

Semanti, B., Rama, A., Falguni B., Shie-Ming P., *et al*.(2010) Iridium assisted S-H and C-H activation of benzaldehyde thiosemicarbazones. Synthesis, structure and electrochemical properties of the resulting complexes. *Inorg. Chim. Acta.*, 363, 2848-2856

Slater, A.F.G., Cerami, A. (1992) Inhibition by chloroquine of a novel haem polymerase enzyme activity in malaria trophozoites. *Nature*, 355: 167–9.

Sulekh, C. Lokesh, K. Gupta., E.P.R. (2005) Mass, IR, electronic, and magnetic studies on copper(II) complexes of semicarbazones and thiosemicarbazones, *Spectrochim. Acta Part A*., 61, 269-275 .

Rey, S.,Gómez,E., Muñoz-Cimadevilla, H., Hevia, D., (2018). Fast and Accurate Electrochemical Measurement of Total Antioxidant Capacity as an Alternative to Spectrophotometrical Methods. *Biomed J Sci & Tech Res.* 21; 1-3

Thangadurai T.D. and Natarajan K. (2001). Tridentate Schiff base complexes of ruthenium(III) containing ONS/ONO donor atoms and their biocidal activites. *Transition Metal Chemistry*, 26, 717-722

Vojinović-Ješić LJ. S., Leovac V. M., Lalović M. M., Češljević V.I., JovanovićLj. S., Rodić M. V., Divjaković V. (2011). Transition metal complexes with thiosemicarbazide-based ligands. Part 58. Synthesis, spectral and structural characterization of dioxovanadium(V) complexes with salicyl aldehyde thiosemicarbazone, *J. Serb. Chem. Soc.* 76 (6), 865–877.

Wiles D.M., Gingras BA, Suprunchuk T. (1967). The C=S stretching vibration in the infrared spectra of some thiosemicarbazones. *Canadian Journal of Chemistry*, 45(5), 469-473.

Summary/Sažetak

Sintetiziran je kompleks željezo(III) salicilaldehid tiosemikarbazon formule $Na[Fe(STSC)_2]$. Ligand (SCT) pripremljen je u reakciji kondenzacije salicilaldehida sa tiosemikarbazidom. $Na[Fe(STSC)_2]$ sintetiziran je u reakciji $FeCl_3$ sa ligandom na bazi tiosemikarbazida sa ONS donorskim atomima. Kompleks je formulisan i okarakterisan masenom spektrometrijom, infracrvenom i UV/Vis spektroskopijom. Podaci su pokazali formiranje metal:ligand kompleksa u stehiometrijskom odnosu 1:2. Ligand je koordiniran kao ONS tridentatni dianion preko atoma kisika nakon deprotoniranja fenolne OH-grupe, azometinskog atoma azota i atoma sumpora u tiolnom obliku poslije deprotoniranja tiosemikarbazidnog ostatka. Određena je antioksidativna aktivnost, gde ligand pokazuje značajnu aktivnost, dok kompleks u maloj koncentraciji, nije pokazao gotovo nikakvu aktivnost.

Glasnik hemičara i tehnologa Bosne i Hercegovine

Bulletin of the Chemists and Technologists of Bosnia and Herzegovina

2020

55

Print ISSN: 0367-4444
Online ISSN: 2232-7266

Original Scientific Article
DOI: https://doi.org/10.35666/ghtbh.2020.55.04
19-24
UDC: 577.1:547.963.4

Peroxidase activity of hemoglobin and heme destruction in the presence of hydrogen peroxide and CT-DNA

Galijašević, S.,[a,*], Muhidinović, M.[b], Grizić, S.[a]

[a]*Sarajevo School of Science and Technology, Sarajevo Medical School, Sarajevo, Bosnia and Herzegovina*
[b]*L'UFR de Chimie, Sorbonne Université, Paris, France*

Article info
Received: 10/08/2020
Accepted: 21/10/2020

Keywords:
hemoglobin
heme
peroxidase
oxidative stress

***Corresponding author:**
Semira Galijasevic
E-mail: semira.galijasevic@ssst.edu.ba
Phone: 00 387-61-410-878

Abstract: The aim of this study was to investigate the peroxidase activity of Hb with different concentrations of hydrogen peroxide and compare it with hypochlorous acid effect on Hb. Hypochlorous acid at higher concentrations decomposed Hb and heme, releasing fee iron ion from the metal center. High concentrations of hydrogen peroxide switched the peroxidase activity of Hb towards the partial Hb and heme destruction. Heme alone was degraded showing that the Hb conformation and protein environment protects Hb from the distraction in the presence of highly increased hydrogen peroxide concentration that occurs as a result of oxidative stress. In the presence of CT-DNA acted inhibition of the peroxidase activity of Hb was observed signaling inhibited hydrogen peroxide consumption.

INTRODUCTION

Hemoglobin (Hb) has an important role in human body as the oxygen-carrying metalloprotein, transporting oxygen from the lungs to the organs, cells, and tissues, where it releases O_2. The oxygenation and deoxygenation processes are highly controlled by the allosteric regulation with the relaxed (R) state between with the high oxygen affinity, and the tense (T) state having the low oxygen affinity, (Schechter, 2008) In addition to its mayor role as oxygen carrier, Hb also performs a number of other functions in biological systems. Hemoglobin is involved in nitric oxide and bicarbonate transport, neutrophile degranulation process, blood coagulation, regulation of a blood pressure, renal absorption, cellular oxidant detoxification and hydrogen peroxide catalytic process. As an example, deoxy-Hb can also show, under defined reaction condition, a nitrite reductase activity thus been involved in compensatory vasodilation in connection with nitric oxide regulation.

A heme (ferroprotoporphyrin IX) is a prostetic group of a number of heme proteins and is noncovalently bonded with each subunit in the space created between the helices in the hydrophobic pocket. The protoporphyrin IX consists of four pyrrole rings linked in a heterocyclic ring system. The Fe(II) is coordinated to the four nitrogen groups of protoporphyrin. The nitrogen atom of proximal histidine is coordinated to the iron from the bottom of the plane and the molecular oxygen binds to the iron on the opposite side.

Despite its significant biological role, under condition of oxidative stress, Hb can become toxic if it is released from erythrocytes. (Rifkind, Mohanty, Nagababu, 2015). This toxicity appeared to be caused by oxidative reactions catalyzed by Hb molecule. As a result, damage to surrounding tissues including biomolecules such as proteins, nucleic acids and lipids occurs (Alayash, Patel, Cashon, 2001). One of the reasons for the hemoglobin toxicity is its susceptibility to oxidation and autoxidation reactions. (Nagababu, Rifkind, 2004). In addition, in the presence of oxidative stress (i.e. high production of free radicals and hydrogen peroxide), heme metal center from hemoglobin is released in the surrounding environment generating more reactive oxygen species and, depending on the reaction condition, releasing free Fe(II). Free Fe(II) is sequestered and stored in ferritin through the tight control of ferritin synthesis in response to cellular iron status. Under extreme conditions, heme destruction is initiated, and excess of free iron is released in the surrounding environment, catalyzing the further formation of free radicals and amplifying host tissue damage (Nagababu, Chrest, Rifkind, 2003). Free Fe(II) can cause vasodilation and as result hypotension and metabolic acidosis will occurs.

Iron damage to mitochondria by lipid peroxidation pathway results in renal and hepatic damage. (Ong, Halliwell, 2004; Trinder, Fox Vautier *et al*., 2002). The major source of hydrogen peroxide in the physiological system is the cellular respiratory burst that generates reactive oxygen species (ROS). This is oxygen dependent process where membrane-bound NADPH oxidase, catalyzes the reduction of molecular oxygen to the reactive oxygen intermediate, superoxide that in the presence of superoxide dismutase (SOD) produces hydrogen peroxide (H_2O_2). Other source of hydrogen peroxide productions in the endothelium are vascular NADPH oxidase, xanthine oxidase (XO), uncoupled endothelial nitric oxide synthase (eNOS) and mitochondrial overproduction of reactive oxygen species. Hb reacts with low H_2O_2 concentrations producing Compound II (○̣HbFe^{4+}=O) (Reactions 1, 2, 3,).

$$HbFe^{2+}\,O_2 + H_2O_2 \rightarrow HbFe^{4+}{=}O + H_2O + O_2 \quad (1)$$
$$HbFe^{4+}{=}O + e^- + 2H^+ \rightarrow HbFe^{3+} + H_2O \quad (2)$$
$$HbFe^{3+} + H_2O_2 \rightarrow ○̣HbFe^{4+}{=}O + H_2O \quad (3)$$

Increased hydrogen peroxide concentration can occur in biological systems during various inflammatory events. Endogenous H_2O_2 produced by neutrophils also has an important role in microbial killing. Less is known that bacteria can also produce H_2O_2 that has an effect on host-microbial interactions. For example, streptococci, pneumococci and lactobacilli due to the structural components-flavoproteins, use molecular oxygen to convert to hydrogen peroxide. Catalase is not present in these microbes, allowing accumulation of hydrogen peroxide. It is known that *S. pneumoniae* infection causes increased production of H_2O_2, up to millimolar concentration (Loose, Hudel, Zimmer, *et al*. 2015; Pericone, Parck, Imlay, *et al*., 2003).

Produced hydrogen peroxide then can serve as a substrate for the number of heme proteins or can be directly sequestered by Hb and incite the heme destruction and free Fe(II) release. Thus, knowing exact mechanism of heme release from hemoglobin and its activity in the presence of different concentrations of H_2O_2 is important since it can explain its determinant role in biological systems especially during the increased oxidative stress. Here we studied the reaction between human Hb (oxy-Hb) with increasing hydrogen peroxide concentrations using spectroscopic methods. We examined the reaction between heme and hydrogen peroxide using spectroscopic method and electrophoresis. Since hypochlorous acid (HOCl) is a strong oxidant and antimicrobial agent in the biological systems that can oxidized a number of biological molecules inflicting host tissue injury, we analyzed the reactions of Hb and heme with different HOCl concentrations. As control, Calf thymus DNA (CT-DNA) was used to test whether it can mitigate toxicity caused by degradation of Hb or heme.

EXPERIMENTAL

Chemicals

All chemicals used were of the highest purity grade and used without further purification. Sodium hypochlorite (NaOCl), heme, human hemoglobin (Hb), dimethylsulfoxide (DMSO), CT-DNA were obtained from Sigma Aldrich (St. Louis, MO, USA).

Absorbance measurements.

The absorbance spectra were recorded using Thermofisher Biosystems UV–visible spectrophotometer at 25°C, and in phosphate buffer at pH 7.2. Fixed concentrations of Hb and heme were prepared and increasing concentration of H_2O_2 added to the solution (10-400 μM). Absorbance spectra were then recorded from 300 to 700 nm. All solutions were prepared fresh before the absorbance measurements.

Agarose gel electrophoresis

Solutions containing the CT-DNA and the Hb were incubated in the presence or absence of H_2O_2 at room temperature. Aliquots were taken and loaded onto 1% agarose gel. Electrophoresis was carried out in TBE buffer (1 M Tris base, 1 M boric acid, and 0.05 M Na_2EDTA, pH 8). The staining of gel was done by ethidium bromide. DNA Step Ladder (50 bp) was used in experiment that contained 17 fragments consisting of 50 bp repeats from 50 to 500 bp, 100 bp repeats from 600 to 900 bp, and 1 kb repeats from 1 to 3 kb.

HOCl solution preparation.

Stock solution of HOCl was prepared by mixing 1 ml of sodium hypochlorite (NaOCl) aqueous solution to 40 ml of 154 mM NaCl. The value of the pH was set at 3 by addition of HCl solution. To convert all convert active chlorine species to OCl^-, the volume 40 μl of 5M NaOH was added and the concentration of OCl^- was measured spectrophotometrically at 292 nm with molar extinction coefficient of 362 $M^{-1}cm^{-1}$.Since HOCl is very unstable, the stock solution was prepared just before the experiments, and stored on ice. All the dilutions were made from the stock solution by addition of appropriate volumes of 200 mM phosphate buffer, pH 7,2.

CT-DNA solution preparation

Stock DNA solutions were prepared by dissolving needed amount of DNA in 5 mM tris(hydroxymethyl)aminomethane (Tris) buffer, mixed with 50 mM NaCl, pH 7.2.

Hemoglobin solution preparation

Hb solution was prepared by dissolving **5** mg of lyophilized powder in 10 mL of 200 mM phosphate buffer pH 7.2 to prepare 7.9 μM solution. Further dilutions were made with the same phosphate buffer.

Heme solution preparation

Heme stock solution was prepared in DMSO and kept in the dark at 4ºC. Diluted solutions were prepared by addition of a phosphate buffer, pH 7.2. The heme concentrations for each diluted solution was calculated by measuring absorbance at 404 nm using molar extinction coefficient of 170,000M^{-1} cm^{-1}.

RESULTS AND DISCUSSION

The first spectra (Figure 1.) shows the changes in the spectra of Hb after addition of 40 μM H_2O_2. The visible spectrum of Hb shows a typical Soret absorbance peak at 405 nm that is indication of a ferric (III) heme. The absorption spectra of pure Hb exhibits several electronic bands located at 279 nm that are the result of phenyl group of tryptophan and tyrosine residues. Another band at 349 nm (e band) also known as Heme or Soret band is centered at 406 nm with two other bands at 540 and 570 nm (oxy band or Q-band) (Kristinsson, 2002).

It is well known that the appearance of strong Soret band (strongly allowed p–p* electron transition) at 406 nm in absorption spectra confirms Hb in its native form. This band is assigned to the heme group. Heme is deeply inserted in the hydrophobic pocket that is created from the protein's back bone through appropriate folding (Khan, Quigley, 2013).

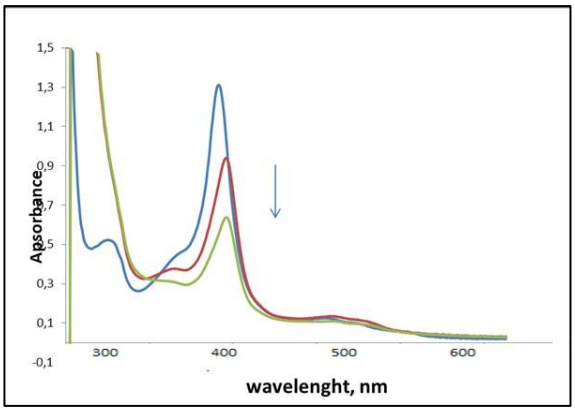

Figure1: The absorption spectra of Hb after addition of 40 μM hydrogen peroxide in phosphate buffer, pH=7.2

Any changes in Soret band are correlated to the changes in the heme microenvironment. After addition of H_2O_2 solution shift in Soret band and intensity was observed. Soret band shifted to 416 nm, but absorbance intensity was lowered. This can be explained by formation of Hb-Fe(IV)=O (Compound II) with a Soret band shifted to 418 nm and with less intensity due to the lower extinction coefficient. The solution of Hb was next incubated with H_2O_2 μM where final concentration of H_2O_2 was 400 μM and decrease in the absorbance was followed over time. (Figure 2).

Increasing concentration of H_2O_2 caused significant Hb heme decomposition that is confirmed by the loss of the intensity of the Soret peak. Incubation of Hb with 400 μM of H_2O_2 caused 70% decrease in the Soret band that after a time decayed indicating heme destruction due to the changes in the heme microenvironment that can be associated with protein aggregation and free iron release. (Maitra, Andreana et al., 2011). As a control, the spectral changes of Hb in the presence of HOCl that can completely oxidize the heme structure of Hb were monitored over time.

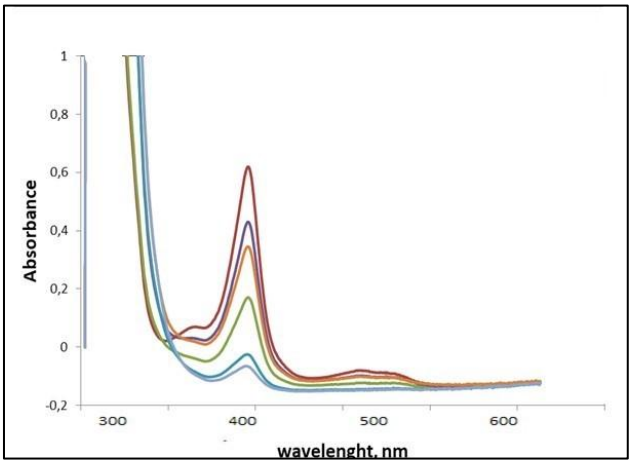

Figure2: The absorption spectra of Hb after addition of 400 μM hydrogen peroxide, in phosphate buffer, pH=7.2

As expected, after addition on a increments of HOCl (10, 20, 40, 80 μM), almost complete flattening of the Soret peaks was observed after 10 minutes indicating complete destruction of the heme structure in Hb (Figure 3.)

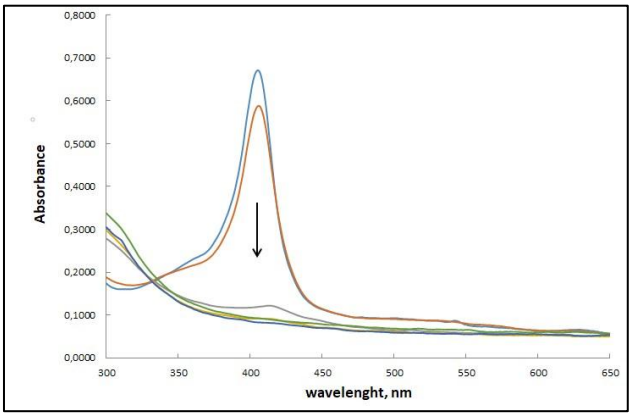

Figure 3: The absorption spectra of Hb obtained by titration with HOCl (5, 10, 20, 40, 80 μM)

Comparing the obtained spectra with ones where Hb changes were observed in the presence of H2O2, it is clear that HOCl directly affect heme environment without formation of Compound II. Apparently HOCl directly cleave the covalent bonds of heme protoporphyrine with protein structure of Hb. Reaction of H_2O_2 with Hb follows peroxidase catalytic mechanism, thus giving the controlled decomposition of Hb. The peroxidase activity of Hb promotes the formation of free radicals and oxidative stress that leads to the modification of biomolecules. Interactions of Hb with CT-DNA were tested in the presence of H_2O_2. Affinity of different forms of hemoglobin for double-stranded DNA was observed earlier (Tan, Cheng, Webber et al., 2005). More recently, a hemoprotein such as myeloperoxidase was detected to form MPO-DNA complexes in the process of NET-osis that is a characteristic response to severe inflammation. The

exact nature of the complex and its role in the defense system is still unknown. Data clearly showed the interactions between the heme proteins and the DNA double helix. Structurally, it is necessary for heme moiety to change the conformation in order to allowed nucleobase oxidation. The presence of H_2O_2 near the heme center and its role as a substrate for the heme center could block and control heme-DNA interaction. Figure 4 shows the absorption spectra of Hb after addition of 40 μM, in phosphate buffer, pH=7.2 with an addition of CT-DNA solution, 1 μM.

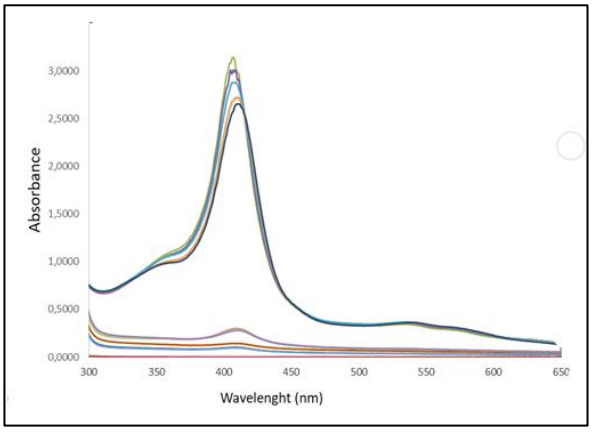

Figure 4. The absorption spectra of Hb after addition of 40 μM hydrogen peroxide, in phosphate buffer, pH=7.2 with an addition of ctDNA solution, 1 μM.

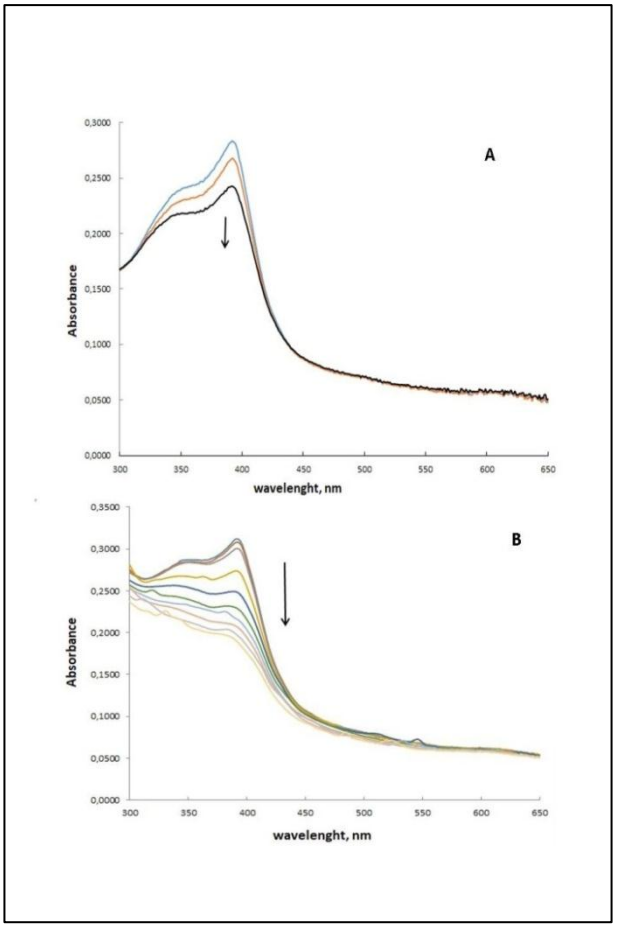

Figure 5. The absorption spectra of heme after addition of A.) 40 μM hydrogen peroxide, and B.) 400 μM hydrogen peroxide in phosphate buffer, pH=7.2

Upon addition of low concentration of H_2O_2 shift in Soret absorbance was observed concomitant with Compound II formation, however, intensity of the Soret absorbance was not significantly lowered when compared with the Soret peak in the absence of ctDNA. This clearly demonstrates that the heme of Hb does not consume H_2O_2 completely due to the blocked heme site. Clearly, molecule of CT-DNA acted as an inhibitor of the peroxidase activity of Hb. In order to test for the effect of the protein environment around heme structure, absorbance spectra of pure heme in the presence of H_2O_2 and HOCl were monitored and compared with those of Hb. (Figure5.)

Heme was completely decomposed upon addition of HOCl (data not shown). In reaction with H_2O_2 the decrease of the typical broad Soret band at 384 nm was observed. Addition of 400 μM of H_2O_2 lowered the absorbance even more and Soret band disappearance was observed indicating the heme decomposition. Clearly, the protein environment close to the heme pocket of Hb plays a role in the peroxidase activity of Hb.
Analysis of possible interactions between DNA and Hb that was incubated H_2O_2 was tested by agarose gel electrophoresis. (Figure 6).

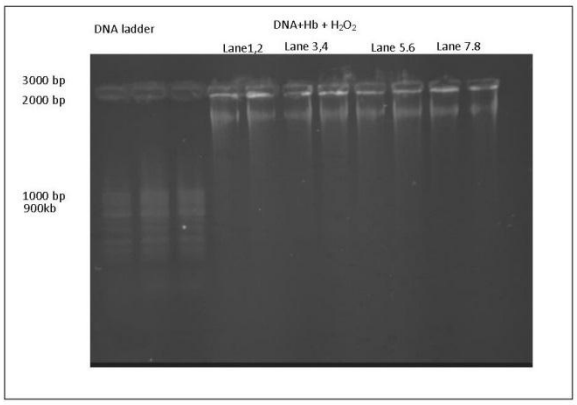

Figure 6 . Gel electrophoresis showing the intensity band of ctDNA in the absence and presence of Hb with various hydrogen peroxide concentrations (lane1,2: 20 μM, lane 3,4: 40 μM, lane 5.6.:100 μM and lane 7.,8: 400 μM)

Lane 1 was untreated DNA alone, while lanes 2–4 ctDNA mixed with Hb and a different concentrations H_2O_2 (20, 40, 100 and 400 μM). Heme inhibited ctDNA fragmentation regardless of H_2O_2 concentrations confirming the possible interactions with the Hb and inhibition of its peroxidase activity. Possible aggregation of protein with ct DNA could explain electrophoretic behavior. In any case, the peroxidation activity of Hb was apparently inhibited.

CONCLUSIONS

The destruction of hemoprotein heme in any extent is a process that can be extremely toxic for surrounding environment. Free iron accumulation has the ability to participate in the production of free radicals via Fenton reaction. Hb reaction with H_2O_2 that follows the

peroxidase mechanism was not responsible for the complete heme destruction even at the higher concentration unlike highly reactive HOCl. Rather, Hb, in the presence of H_2O_2 showed formation of Compound II indicating classic peroxidase behavior. Mechanism of its peroxidase activity is highly controlled by the protein conformation rather than heme iron since heme alone was partially destructed by the increased in H_2O_2concentration. CT-DNA partially blocked the peroxidase activity of Hb, with a possible formation of heme-DNA adduct. These interconnecting mechanisms indicate the highly controlled environment even in the cases of elevated oxidative stress and might act in a protective manner. Further studies are needed to decipher the exact nature of these interactions.

REFERENCES

Beck, J. J. Chou, S. C. (2007). The Structural Diversity of Phthalides from the Apiaceae. *Journal of Natural Product*, *70 (5)*, 891-900.

Alayash, A. I., Patel, R. P., Cashon, R. E. (2001) Redox reactions of hemoglobin and myoglobin: biological and toxicological implications. *Antioxidants & Redox Signaling*, *3*(2), 313–327.

Khan, A. A., Quigley, J. G. (2013) Heme and FLVCR-related transporter families SLC48 and SLC49. *Molecular Aspects of Medicine*, *34*(2-3), 669-682.

Kristinsson, H. G. (2002) Acid-induced unfolding of flounder hemoglobin: evidence for a molten globular state with enhanced pro-oxidative activity. *Journal of Agricultural and Food Chemistry*, *50*(26), 7669-7676.

Loose, M., Hudel, M., Zimmer, K. P. (2015) Pneumococcal hydrogen peroxide-induced stress signaling regulates inflammatory genes. *Journal of Infectious Diseases*, *211*(2), 306-316.

Maitra, D., Byun, J., Andreana, P. R., Ibrahim Abdulhamid, I., Diamond, M., Saed, M. G., Pennathur, S., Abu-Soud, M. H. (2011) Reaction of hemoglobin with HOCl: mechanism of heme destruction and free iron release. *Free Radicals in Biology and Medicine*, *51*(2), 374–38.

Nagababu, E., Chrest, F., Rifkind, J. (2003). Hydrogen-peroxide-induced heme degradation in red blood cells: The protective roles of catalase and glutathione peroxidase. *Biochimica et biophysica acta*. *1620*(1-3), 211-7.

Nagababu, E., Rifkind, J. M. (2004) Heme degradation by reactive oxygen species. *Antioxidants & Redox Signal*, *6*, 967–978.

Ong, W. Y., Halliwell, B. (204) Iron, Atherosclerosis, and Neurodegeneration: A Key Role for Cholesterol in Promoting Iron-Dependent Oxidative Damage? *Annals of the New York Academy of Sciences*, *1012*, 51–64.

Pericone, C., Park, S., Imlay, J., Weiser, J. (2003) Factors Contributing to Hydrogen Peroxide Resistance in *Streptococcus pneumoniae* Include Pyruvate Oxidase (SpxB) and Avoidance of the Toxic Effects of the Fenton Reaction. *Journal of Bacteriology*, *185*(23), 6815-6825.

Rifkind, J. M., Mohanty, J. G., Nagababu, E. (2015) The pathophysiology of extracellular hemoglobin associated with enhanced oxidative reactions. *Frontiers in Physiology*, *5*, 500.

Schechter, A. N. (2008) Hemoglobin research and the origins of molecular medicine. *Blood*, *112*, 3927–3938

Tan, W. B., Cheng, W., Webber, A., Bhambhani, A., Duff, M. R., Kumar, C. V., McLendon, G. L. (2005). Endonuclease-like activity of heme proteins. *JBIC Journal of Biological Inorganic Chemistry*, *10*(7), 790–799.

Trinder, D., Fox, C., Vautier, G., Olynyk, J. K. (2002) Molecular pathogenesis of iron overload. *Gut*, *51*, 290–295.

Summary/Sažetak

Hemoglobin je protein sa hem centrom, tetramer koji se sastoji od četiri podgrupe proteinskih globina i četiri proteinske skupine hema. Najvažnija funkcija Hb je isporuka kisika iz pluća u periferno tkivo za stanični metabolizam. U uvjetima oksidativnog stresa mogući su načini uništavanja hema ili stvaranja drugih viših oksidativnih stanja. Cilj ove studije bio je istražiti aktivnost peroksidaze Hb s različitim koncentracijama vodikovog peroksida. Visoke koncentracije vodikovog peroksida preusmjerile su aktivnost peroksidaze Hb prema djelomičnom uništavanju Hb hema. Sam hem je degradiran, pokazujući da konformacija Hb i proteinsko okruženje štite Hb od distrukcije u prisustvu visoko povećane koncentracije vodikovog peroksida koja nastaje kao rezultat oksidativnog stresa.

INSTRUCTIONS FOR AUTHORS

GENERAL INFORMATION

Bulletin of the Chemists and Technologists of Bosnia and Herzegovina (Glasnik hemičara i tehnologa Bosne i Hercegovine) is a semiannual international journal publishing papers from all fields of chemistry and related disciplines.

Categories of Contributions

1. *Original Scientific Papers* – (about 10 typewritten pages) report original research which has not been published previously, except in a preliminary form. The paper should contain all the necessary information to enable reproducibility of the described work.
2. *Short Communications* – (about 5 typewritten pages) describing work that may be of a preliminary nature but which merits immediate publication.
3. *Notes* – (about 3 typewritten pages) report unpublished results of short, but complete, original research or describe original laboratory techniques.
4. *Reviews* – (about 30 typewritten pages) present a concise and critical survey of a specific research area. Generally, these are prepared by the invitation of the Editor.
5. *Book and Web Site Reviews* – (about 2 typewritten pages).
6. *Extended Abstracts* – (about 2 typewritten pages) of Lectures given at international meetings.

Reviewing the Manuscript

All contributors are evaluated according to the criteria of originality and quality of their scientific content, and only those deemed worthy will be accepted for publication. To facilitate the reviewing process, authors are encouraged to suggest three persons competent to review their manuscript. Such suggestions will be taken into consideration but not always accepted.

The Editor-In-Chief and Editors have the right to decline formal review of a manuscript when it is deemed that the manuscript is:

1. on a topic outside the scope of the Journal;
2. lacking technical merit;
3. of insufficient novelty for a wide international readership;
4. fragmentary and providing marginally incremental results; or
5. is poorly written.

Proofs

When a manuscript is ready for printing, the corresponding author will receive a PDF-formatted manuscript for proof reading, which should be returned to the journal within one week. Failure to do so will be taken as the authors are in agreement with any alteration which may have occurred during the preparation of the manuscript.

Copyright

Subscribers may reproduce tables of contents or prepare lists of articles including abstracts for internal circulation within their institutions. Permission of the Publisher is required for resale or distribution outside the institution and for all other derivative works, including compilations and translations.

Professional Ethics and Publication Policy

The journal expects the Editors, Referees and authors to adhere to the well-known standards of professional ethics. Authors are responsible for the factual accuracy of their contributions. Submission of the paper commits the author not to submit the same material elsewhere. Referees should act promptly. If certain circumstances preclude prompt attention to the manuscript at the time it is received, the non-received manuscript should be returned immediately to the Editor or the Referee should contact the Editor for possible delay of the report submission date. The Editor accepts full responsibility for his decisions on the manuscripts.

PREPARATION AND SUBMISSION OF MANUSCRIPT

Cover Letter

Manuscripts must be accompanied by a cover letter in which the type of the submitted manuscript. It should contain:

1. full name(s) of the author(s),
2. mailing address (address, phone and fax numbers, e-mail) of the author to whom correspondence should be addressed,
3. title of the paper (concise, without any abbreviations),
4. type of contribution,
5. a statement that the article is original and is currently not under consideration by any other journal or any other medium, including preprints, electronic journals and computer databases in the public domain, and
6. the names, full affiliation (department, institution, city and country), and
7. e-mail addresses of three potential Referees.

Contributors from Bosnia and Herzegovina should provide the name and full affiliation of at least one Referee from abroad.

Authors are fully encouraged to use ***Cover Letter Template.***

Manuscript preparation

The submitted articles must be prepared with Word for Windows. Manuscripts should be typed in English (either standard British or American English, but consistent throughout) with 1.5 spacing (12 points Times New Roman; Greek letters in the character font Symbol) in A4 format leaving 2.5 cm for margins. Authors are fully encouraged to use ***Manuscript Template***.

All contributions should be written in a style that addresses a wider audience than papers in more specialized journals. Manuscripts with grammar or vocabulary deficiencies are disadvantaged during the scientific review process and, even if accepted, may be returned to the author to be rewritten in idiomatic English. The authors are requested to seek the assistance of competent English language expert, if necessary, to ensure their English is of a reasonable standard. The journal maintains its policy and takes the liberty of correcting the English of manuscripts scientifically accepted for publication.

Tables and figures and/or schemes should not be embedded in the manuscript but their position in the text indicated. In electronic version (Word.doc document) tables and figures and/or schemes should follow the text, each on a separate page. Please number all pages of the manuscript including separate lists of references, tables and figures with their captions.

IUPAC and International Union of Biochemistry and Molecular Biology recommendations for the naming of compounds should be followed.

SI units, or other permissible units, should be employed. The designation of physical quantities should be in Times New Roman font. In text, graphs, and tables, brackets should be used to separate the designation of a physical quantity from the unit. Please do not use the axes of graphs for additional explanations; these should be mentioned in the figure captions and/or the manuscript (example: “pressure at the inlet of the system, kPa” should be avoided).

Percents and *per mills*, although not being units in the same sense as the units of dimensioned quantities, can be treated as such. Unit symbols should never be modified (for instance: w/w %, vol.%, mol.%) but the quantity measured has to be named, *e.g.* mass fraction, w=95 %; amount (mole) fraction, x=20 %.

Latin words, as well as the names of species, should be in *italic*, as for example: *i.e., e.g., in vivo, ibid, Artemisia annua* L., *etc*. The branching of organic compound should also be indicated in *italic*, for example, *n*-butanol, *tert*-butanol, *etc*.

Decimal numbers must have decimal points and not commas in the text (except in the Bosnian/Croatian/Serbian abstract), tables and axis labels in graphical presentations of results. Thousands are separated, if at all, by a comma and not a point.

Structure of the Manuscript

The manuscript must contain, each on a separate page, the title page, abstract in English, (abstract in Bosnian/Croatian/Serbian), graphical abstract (optional), main text, list of references, tables (each table separately), illustrations (each separately), and legends to illustrations (all on the same page).

1. ***Title page*** must contain: the title of the paper (bold letters), full name(s) of the author(s), full mailing addresses of all authors (italic), keywords (up to 6), the phone and fax numbers and the e-mail address of the corresponding author.
2. A one-paragraph ***abstract*** written of 150–200 words in an impersonal form indicating the aims of the work, the main results and conclusions should be given and clearly set off from the text. Domestic authors should also submit, on a separate page, a Summary/Sažetak. For authors outside Bosnia and Herzegovina, the Editorial Board will provide a Bosnian/Croatian/Serbian translation of their English abstract.
3. Authors are encouraged to submit a ***graphical abstract*** that describes the subject matter of the paper. It should contain the title of the paper, full name(s) of the author(s), and graphic that should be no larger than 11 cm wide by 5 cm tall. Authors are fully encouraged to use ***Graphical Abstract Template.***
4. ***Main text*** should have the following form:
   - ***Introduction***should include the aim of the research and a concise description of background information and related studies directly connected to the paper.
   - ***Experimental*** section should give the purity and source of all employed materials, as well as details of the instruments used. The employed methods should be described in sufficient detail to enable experienced persons to repeat them. Standard procedures should be referenced and only modifications described in detail.
   - ***Results and Discussion***should include concisely presented results and their significance discussed and compared to relevant literature data. The results and discussion may be combined or kept separate.
   - The inclusion of a ***Conclusion***section, which briefly summarizes the principal conclusions, is highly recommended.
   - ***Acknowledgement*** (optional).
   - Please ensure that every ***reference*** cited in the text is also present in the reference list (and *vice versa*). Unpublished results and personal communications are not recommended in the reference list, but may be mentioned in the text. If these references are included in the reference list they should follow the standard reference style of the journal and should include a substitution of the publication date with either "Unpublished results" or "Personal communication" Citation of a reference as "in press" implies that the item has been accepted for publication. As a minimum, the full URL should be given and the date when the reference was last accessed. Any further information, if known (DOI, author names, dates, reference to a source publication, etc.), should also be given. No more than 30 references should be cited in your manuscript.

     In the text refer to the author's name (without initials) and year of publication (e.g. "Steventon, Donald and Gladden (1994) studied the effects..." or "...similar to values reported by others (Anderson, Douglas, Morrison, *et al.*, 1990)..."). Type the names of the first three authors at first citation. At subsequent citations use first author *et al.* The list of references should be arranged alphabetically by

authors' names and should be as full as possible, listing all authors, the full title of articles and journals, publisher and year.

Examples of ***reference style***:

a) Reference to a journal publication:
   Warren, J. J., Tronic, T. A., Mayer, J. M. (2010). Termochemistry of proton-coupled electron transfer reagents and its implications. *Chemical Reviews*, *110 (12)*, 6961-7001.
b) Reference to a book:
   Corey, E. J., Kurti, L. (2010). *Enantioselective chemical synthesis*. (1st Ed.) Direct Book Publishing, LLC.
c) Reference to a chapter in an edited book:
   Moody, J. R., Beck II, C. M. (1997). Sample preparation in analytical chemistry. In Setlle, F. A. (Ed.), *Handbook of instrumental techniques for analytical chemistry*. (p.p. 55-72). Prentice Hall.
d) Reference to a proceeding:
   Seliskar, C. J., Heineman, W.R., Shi, Y., Slaterbeck, A.F., Aryal, S., Ridgway, T.H., Nevin, J.H. (1997). *New spectroelectrochemical sensor*, in Proceedings of 37th Conference of Analytical Chemistry in Energy and Technology, Gatlinburg, Tenesee, USA, p.p. 8-11.
e) Patents:
   Healey, P.J., Wright, S.M., Viltro, L.J., (2004).*Method and apparatus for the selection of oral care chemistry*, The Procter & Gamble Company Intellectual Property Division, (No.US 2004/0018475 A1).
f) Chemical Abstracts:
   Habeger, C. F., Linhart, R. V., Adair, J. H. (1995). Adhesion to model surfaces in a flow through system. *Chemical Abstracts,* CA 124:25135.
g) Standards:
   ISO 4790:1992. (2008). *Glass-to-glass sealings - Determination of stresses*.
h) Websites:
   Chemical Abstract Service, www.cas.org, (18/12/2010).

- ***Tables*** are part of the text but must be given on separate pages, together with their captions. The tables should be numbered consequently in Latin numbers. Quantities should be separated from units by brackets. Footnotes to tables, in size 10 font, are to be indicated consequently (line-by-line) in superscript letters. Tables should be prepared with the aid of the Word table function, without vertical lines. Table columns must not be formatted using multiple spaces. Table rows must not be formatted using Carriage returns (enter key; ↵ key). Tables should not be incorporated as graphical objects.
- ***Figures and/or Schemes*** (in high resolution) should follow the captions, each on a separate page of the manuscript. High resolution illustrations in TIF or EPS format (JPG format is acceptable for colour and greyscale photos, only) must be uploaded as a separate archived (.zip or .rar) file.

Figures and/or Schemes should be prepared according to the artwork instructions.

- ***Mathematical and chemical equations*** must be numbered, Arabic numbers, consecutively in parenthesis at the end of the line. All equations should be embedded in the text except when they contain graphical elements (tables, figures, schemes and formulae). Complex equations (fractions, inegrals, matrix…) should be prepared with the aid of the Word Equation editor.

Artwork Instructions

Journal accepts only TIF or EPS formats, as well as JPEG format (only for colour and greyscale photographs) for electronic artwork and graphic files. MS files (Word, PowerPoint, Excel, Visio) are NOT acceptable. Generally, scanned instrument data sheets should be avoided. Authors are responsible for the quality of their submitted artwork.

Image quality: keep figures as simple as possible for clarity - avoid unnecessary complexity, colouring and excessive detail. Images should be of sufficient quality for the printed version, i.e. 300 dpi minimum.

Image size: illustrations should be submitted at its *final size* (8 cm for single column width or 17 cm for double column width) so that neither reduction nor enlargement is required.

Photographs: please provide either high quality digital images (250 dpi resolution) or original prints. Computer print-outs or photocopies will not reproduce well enough for publication. Colour photographs rarely reproduce satisfactorily in black and white.

The facility exist for color reproduction, however the inclusion of color photographs in a paper must be agreed with Editor in advance.

Reporting analytical and spectral data

The following is the recommended style for analytical and spectral data presentation:

1. ***Melting and boiling points***:
   mp 163–165°C (lit. 166°C)
   mp 180°C dec.
   bp 98°C
   Abbreviations: mp, melting point; bp, boiling point; lit., literature value; dec, decomposition.
2. ***Specific Rotation***:
   $[a]^{23}_{D}$ –222 (*c* 0.35, MeOH).
   Abbreviations: a, specific rotation; D, the sodium D line or wavelength of light used for determination; the superscript number, temperature (°C) at which the determination was made; In parentheses: *c* stands for concentration; the number following *c* is the concentration in grams per 100 mL; followed by the solvent name or formula.

3. ***NMR Spectroscopy***:
   ^{1}H NMR (500 MHz, DMSO-d_6) d 0.85 (s, 3H, CH_3), 1.28–1.65 (m, 8H, 4´CH_2), 4.36–4.55 (m, 2H, H-1 and H-2), 7.41 (d, *J* 8.2 Hz, 1H, ArH), 7.76 (dd, *J* 6.0, 8.2 Hz, 1H, H-1'), 8.09 (br s, 1H, NH).
   ^{13}C NMR (125 MHz, $CDCl_3$) d 12.0, 14.4, 23.7, 26.0, 30.2, 32.5, 40.6 (C-3), 47.4 (C-2'), 79.9, 82.1, 120.0 (C-7), 123.7 (C-5), 126.2 (C-4).
   Abbreviations: d, chemical shift in parts per million (ppm) downfield from the standard; *J*, coupling constant in hertz; multiplicities s, singlet; d, doublet; t, triplet; q, quartet; and br, broadened. Detailed peak assignments should not be made unless these are supported by definitive experiments such as isotopic labelling, DEPT, or two-dimensional NMR experiments.
4. ***IR Spectroscopy***:
   IR (KBr) n 3236, 2957, 2924, 1666, 1528, 1348, 1097, 743 cm^{-1}.
   Abbreviation: n, wavenumber of maximum absorption peaks in reciprocal centimetres.
5. ***Mass Spectrometry***:
   MS *m/z* (relative intensity): 305 (M^+H, 100), 128 (25).
   HRMS–FAB (*m/z*): $[M+H]^+$calcd for $C_{21}H_{38}N_4O_6$, 442.2791; found, 442.2782.
   Abbreviations: *m/z*, mass-to-charge ratio; M, molecular weight of the molecule itself; M^+, molecular ion; HRMS, high-resolution mass spectrometry; FAB, fast atom bombardment.
6. ***UV–Visible Spectroscopy***:
   UV (CH_3OH) l_{max} (log e) 220 (3.10), 425 nm (3.26).
   Abbreviations: l_{max}, wavelength of maximum absorption in nanometres; e, extinction coefficient.
7. ***Quantitative analysis***:
   Anal.calcd for $C_{17}H_{24}N_2O_3$: C 67.08, H 7.95, N 9.20. Found: C 66.82, H 7.83, N 9.16.All values are given in percentages.
8. ***Enzymes and catalytic proteins relevant data:***
   Papers reporting enzymes and catalytic proteins relevant data should include the identity of the enzymes/proteins, preparation and criteria of purity, assay conditions, methodology, activity, and any other information relevant to judging the reproducibility of the results[1]. For more details check Beilstein Institut/STRENDA (standards for reporting enzymology data) commission Web site (http://www.strenda.org/documents.html).

Submission Checklist

The following list will be useful during the final checking of an article prior to sending it to the journal
for review:

- E-mail address for corresponding author,

[1] For all other data presentation not mentioned above please contact Editor for instructions.

- Full postal address,
- Telephone and fax numbers,
- All figure captions,
- All tables (including title, description, footnotes),
- Manuscript has been "spellchecked" and "grammar-checked",
- References are in the correct format for the journal,
- All references mentioned in the Reference list are cited in the text, and *vice versa*.

Submissions

Submissions should be directed to the Editor by e-mail: ***glasnik@pmf.unsa.ba***, or ***glasnikhtbh@gmail.com***. All manuscripts will be acknowledged on receipt (by e-mail) and given a reference number, which should be quoted in all subsequent correspondence.

Glasnik hemičara i tehnologa Bosne i Hercegovine

Bulletin of the Chemists and Technologists of Bosnia and Herzegovina

Print ISSN: 0367-4444
Online ISSN: 2232-7266

Zmaja od Bosne 33-35, BA-Sarajevo
Bosnia and Herzegovina
Phone: +387-33-279-918
Fax: +387-33-649-359
E-mail: glasnik@pmf.unsa.ba
glasnikhtbh@gmail.com

Sponsors

Glasnik hemičara i tehnologa Bosne i Hercegovine

Bulletin of the Chemists and Technologists of Bosnia and Herzegovina

Print ISSN: 0367-4444
Online ISSN: 2232-7266

Zmaja od Bosne 33-35, BA-Sarajevo
Bosnia and Herzegovina
Phone: +387-33-279-918
Fax: +387-33-649-359
E-mail: glasnik@pmf.unsa.ba
glasnikhtbh@gmail.com

www.elektroprivreda.ba/stranica/te-kakanj

FMON
Federalno ministarstvo obrazovanja i nauke

www.fmon.gov.ba

Ministarstvo za obrazovanje, nauku i mlade Kantona Sarajevo

https://mon.ks.gov.ba